National Defence
Research and Development Branch

Défense nationale
Bureau de recherche et développement

CR 97/419

EVALUATION OF CAVITATION EROSION BEHAVIOR OF A LASER SURFACE MELTED EXPERIMENTAL NICKEL ALUMINUM BRONZE

by
K.J. KarisAllen & C.A.Taweel

FACTS Engineering Inc.
P.O. Box 20039
Halifax, Nova Scotia.
Canada B3R 2K9

CONTRACTOR REPORT

Prepared for

Defence Research Establishment Atlantic

Centre de Recherches pour la Défense Atlantique

Canada

National Defence
Research and Development Branch

Défense nationale
Bureau de recherche et développement

CR 97/419

EVALUATION OF CAVITATION EROSION BEHAVIOR OF A LASER SURFACE MELTED EXPERIMENTAL NICKEL ALUMINUM BRONZE

by
K.J. KarisAllen & C.A.Taweel

FACTS Engineering Inc.
P.O. Box 20039
Halifax, Nova Scotia.
Canada, B3R 2K9

Scientific Authority C.V.Hyatt

W7707-6-4270/001/HAL
Contract Number

May 1997

CONTRACTOR REPORT

Prepared for

Defence Research Establishment Atlantic

Centre de Recherches pour la Défense Atlantique

Canada

ABSTRACT

A series of laser surface melted experimental nickel aluminum bronze coupons have been evaluated for cavitation erosion resistance. Duplicate specimens of twenty five differing alloy compositions have been tested in accordance with ASTM G-32. For the materials tested, test results indicate that alloy chemistries with more than 10.7 wt percent Al produce the best resistance to cavitation erosion. The cavitation resistance of alloys with less than 10.7 percent Al can be improved through the addition of Cr. The analysis also indicates that the linear extrapolation method recommended in ASTM G-32 may produce non conservative incubation times for laser surface melted specimens with above average erosion performance.

RÉSUMÉ

Une séries d'éprouvettes expérimentales en bronze au nickel-aluminium ayant subi une fusion superficielle au laser ont été soumises à des essais visant à évaluer leur résistance à l'érosion par cavitation. Deux séries identiques de vingt-cinq alliages de composition variable ont été vérifiées par la méthode décrite dans la norme ASTM G-32. Les résultats des essais montrent que les alliages renfermant plus de 10.7% en poids d'aluminium offrent la meilleure résistance à l'érosion par cavitation. Il est possible d'améliorer la résistance des alliages renfermant moins de 10.7% d'aluminium en ajoutant du chrome. L'analyse a également révélé que la méthode d'extrapolation linéaire recommandée dans la norme ASTM G-32 peut conduire à des temps d'incubation non raisonnables dans le cas des éprouvettes traitées au laser dont la résistance à l'érosion est supérieure à la moyenne.

TABLE OF CONTENTS

1. INTRODUCTION

Over the past several years, the Department of National Defence has been evaluating various means of extending the operational service life of high value components such as Nickel-Aluminum-Bronze (NAB) high pressure hull valves. Condemnation of these valves usually occurs because of stringent dimensional tolerances required around valve seats. Mechanical wear, hydraulic erosion and corrosion combine to cause degradation of these critical areas.

Defence Research Establishment Atlantic (DREA) has identified laser surface modification as a possible means of extending the life of these high value components. Ongoing work at DREA [1-3] and contracted R&D [4,5] supervised by DREA has detailed the processing windows for numerous commercially available candidate materials and processes. To continue advancing the state of the art, DREA/DL recently commissioned the development of a set of new consumable materials for use in the surface modification of NAB materials. A series of test coupons were manufactured for the various consumable chemistries of interest. During the past year, work has been focused on evaluating the corrosion and erosion performance [6] of the candidate chemistries. This report details the testing program for the evaluation of the cavitation erosion resistance of these materials in seawater.

2. TECHNICAL BACKGROUND

There have been numerous devices developed to simulate cavitation erosion. Full scale tests in water tunnels were the first units to be used to test for cavitation resistance. These tunnels were constructed to test and view the cavitation of propellers and other underwater bodies. As the name suggests, this apparatus is a tunnel circuit (usually closed) through which water flows. The test part is placed in the flow to simulate actual cavitation situations. One of the prime benefits of this apparatus is the testing of actual parts under service conditions. The main disadvantage is that the tunnel with its pump is extremely large [7].

Venturi devices are an alternative method of testing for cavitation erosion resistance. The main component of this test device is a venturi section which creates a high velocity - low pressure region in a stream of water. Bubbles form in the low pressure region and then collapse on a test specimen located in a high pressure region downstream. This system is used to compare the relative erosion of different materials under cavitating conditions. Venturi systems require long test times, a large amount of laboratory space and are expensive to construct.

Rotary disc testers are also used to evaluate the cavitation erosion resistance of metallic materials. A rotary tester is normally comprised of a thin disc which is submerged in the test liquid and rotated at high velocity. Small holes are cut in the disc to produce turbulence. Samples of the test material are mounted on the wheel so that the bubbles generated by the holes collapse on them. The complexity of the water flow pattern makes control and adjustment of cavitating parameters difficult.

The vibratory device is probably the most commonly used accelerated cavitation tester due to its simplicity, small size and relatively low cost. A converter which changes a cyclic electrical signal to a cyclic mechanical strain via piezoelectric crystals is used to vibrate a metal horn in the kilohertz frequency range. The vibrating tip of the horn is immersed in the test liquid and bubbles form during the upstroke when the local pressure decreases. During the subsequent downstroke, the pressure increases and the bubbles collapse. The test material is usually connected to the vibrating horn. Thus the vibration of the test material in the liquid causes cavitation. For soft materials which would fail due to the mechanical vibration, a stationary vice is placed under the vibrating horn [8]. This vice holds the test sample under the bubble cloud.

The cavitation device chosen for this study is an ultrasonic vibratory device operating at 20 kHz. This device was chosen over the other cavitators because of its small size, ease of operation and low noise level. A schematic of the ultrasonic unit is shown in Figure 1. The ultrasonic unit consists of four major components: power supply, converter, booster assembly and horn. The power supply is capable of producing an A.C. output with a square waveform at a fixed frequency of 20 kHz. The magnitude of this voltage is controlled by a voltage regulator located on the front of the power unit. This high frequency signal is then sent to the converter. The converter contains a disc shaped piezoelectric crystal which converts the electrical signal to a mechanical vibration. When the alternating voltage from the power supply is applied to the two faces of the crystal disc, the disc expands and contracts with the alternating polarity (since the signal from the power supply alternates at 20 kHz, the disc vibrates at the same frequency.

Inside the converter, the crystal(s) (more than one piezoelectric crystal may be used in a converter) is sandwiched between two pieces of metal. This assembly (crystals and metal pieces) is called an electrostrictive transducer. The entire transducer assembly has a predetermined resonant frequency and the length is such that the assembly, at the applied frequency, vibrates with the nodal point at its end.

The vibration from the converter is transferred to a booster assembly via a tight screw connection between the two parts. A booster is used to accommodate a wide range of final amplitudes at the horn tip. The booster assembly changes the vibration amplitude because of different masses on either side of the central nodal point. (Note that the length of the booster assembly is such that it resonates one-half wavelength at the given frequency). If the mass of the booster is greater on the converter side of the nodal point than on the horn side, then the booster will increase the amplitude of the vibration from the converter. Conversely, if the large mass is on the horn side, the booster will decrease the converter vibration amplitude.

The horn, usually made of titanium, amplifies the vibrational output from the booster. The test specimen can be screwed into the end of the horn. The length of the horn, with the specimen in place, is such that they also resonate at one-half wavelength. This means that the specimen tip is at a maximum vibratory amplitude.

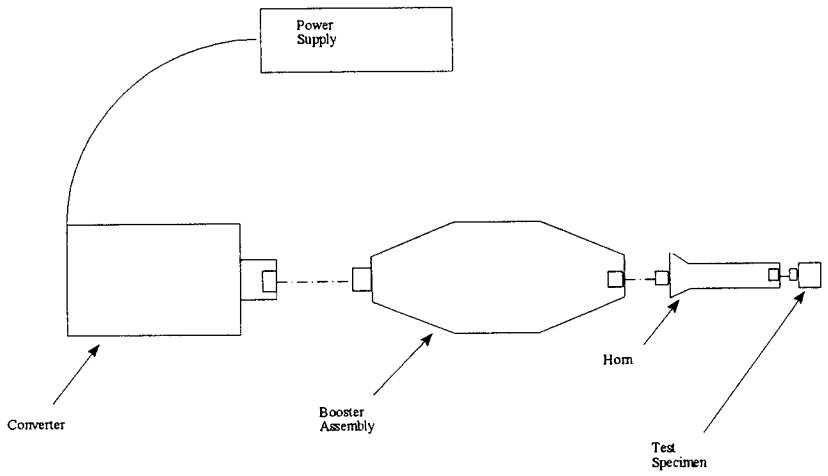

Figure 1 - Schematic representation of ultrasonic testing unit

The entire converter assembly is mounted on a plastic holder which clamps the assembly at the nodal points of the vibration wave. The nodal points are isolated by rubber '0' rings in the booster and converter housing. The back of the holder is equipped with clamps to secure the converter assembly during operation. During testing, the horn tip (with the test specimen attached) is immersed in a flask containing the test liquid.

3. EXPERIMENTAL PROCEDURE

3.1 Experimental Apparatus

Figure 2 shows the experimental test apparatus used. The converter was a Branson Model No. 108 connected to a 184V power supply/function generator. A 1:1 booster was attached between the titanium horn and the converter. The specimens were attached at the lower extremity of the horn which was submerged in seawater during testing.

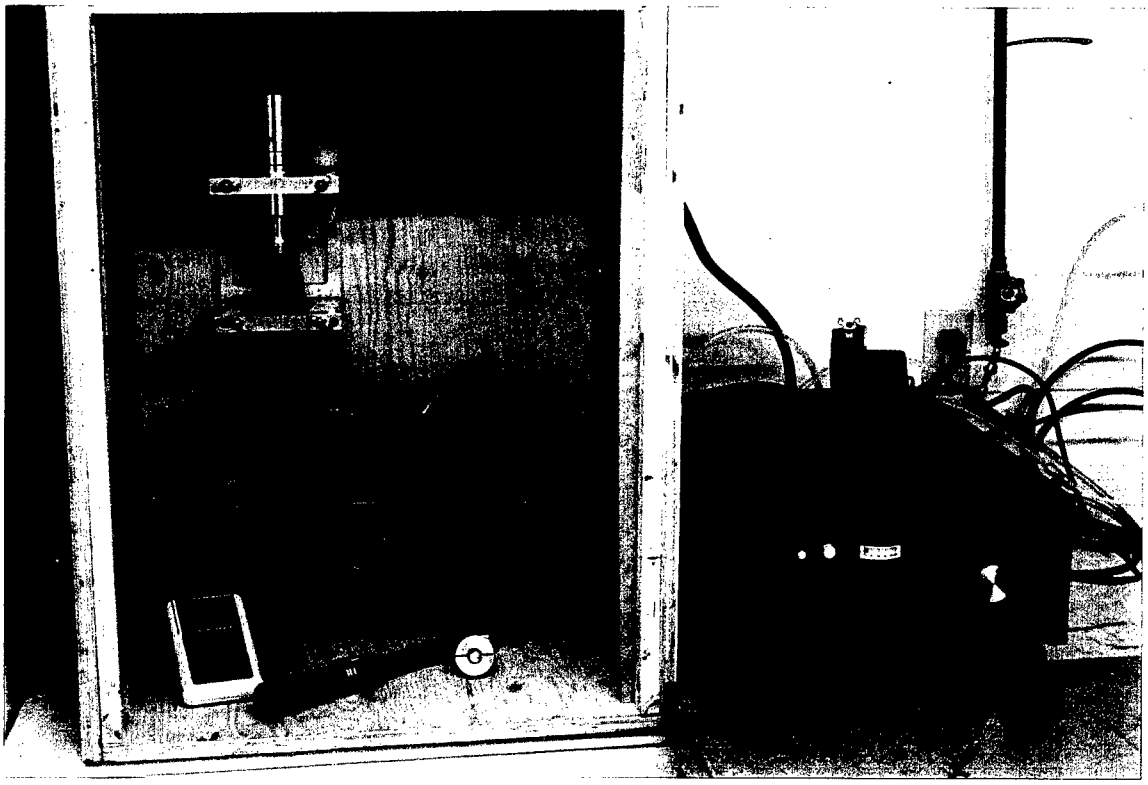

Figure 2 - Experimental test apparatus

During testing, the temperature of the liquid that surrounded the test specimen in the flask increased due to the mechanical action of the horn. This temperature increase necessitated a cooling bath around the flask. The cooling bath consisted of a container of water in which a copper coil connected to a cold water supply was submersed. The coil cooled the bath water and worked in combination with a mechanical stirrer/heater to maintain the liquid testing medium at 25 ^{0}C ± 2 ^{0}C.

A peak to peak amplitude of 0.05 mm was maintained throughout the test. The amplitude of the horn tip was regulated by the booster horn and by the voltage from the power supply. To regulate the amplitude during the test, the voltage corresponding to 0.05 mm was determined using a digital voltmeter. The converter was mounted horizontally so that the end of the

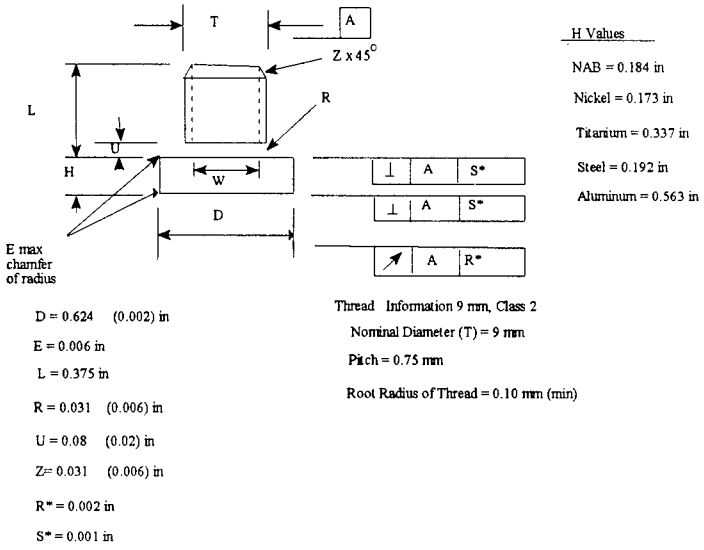

Figure 3 - Dimensional drawings of the specimen configuration.

specimen was viewed under a microscope. A series of voltage readings was taken from the voltmeter and a vernier in the eyepiece was used to measure the corresponding band width or amplitudes. Both ultrasonic test machines employed during this study produced 0.05 mm at a voltage of approximately 153.0 Vdc. Accordingly, the voltage was maintained at between 152 Vdc and 154 Vdc during testing. The operating frequency of the horn was maintained at 20 kHz.

3.2 Test Specimen

Fifty test specimens of the surface treated NAB coupons were provided by DREA/DL. Figure 3 provides the dimensional detail of the specimens manufactured by DREA. Table 1 is a summary of the chemical analysis for the test specimens provided. Prior to testing, each specimen surface was prepared by polishing to 600 grit on emery paper. The specimens were washed with acetone in an ultrasonic bath, rinsed with acetone and blown dry. Specimens were subsequently handled with tongs to ensure a grease free surface. After cleaning, the mass of the specimen was measured to ± 0.1 mg. The samples were stored in a desiccator when not being tested.

3.3 Procedure

For each run, a two liter beaker was filled with naturally occurring seawater and placed in the water bath. A 316 stainless steel specimen was run in the seawater for 30 minutes to stabilize the gas content. The specimen was then screwed into the horn tip and pretorqued to 120 in-lbf with a torque wrench. The test apparatus holder slid vertically on a rod at the back of the cabinet. The holder was positioned so that the face of the test specimen was immersed approximately 10

mm in the test liquid. The power was activated and the voltage adjusted to between 152 Vdc and 154 Vdc.

Test duration was approximately 16-20 hours. For the first half of the test, the specimen was removed from the horn every hour, washed with acetone, blown dry and weighed using an analytical scale. For the second half of the test, this procedure was repeated every two hours. When the test was completed, the weight of the specimen was recorded and the specimen stored in a desiccator.

Table 1 - Chemical analysis for the specimens provided by DREA/DL

Alloy ID No.	Chemical Composition (wt%)						
	Ni	Fe	Mn	Al	Cr	Ti	Zr
1	5.06	6.2	0.35	9.7		2.24	
2	3.6-3.8	5.5	0.96-1.0	10.01			
3	5.0	4.7	1.1	9.1			
4	3.8	3.9	1.0	10.1			
5	6.5	4.6	1.1	9.2			
6	4.7	3.8	1.3	12.2			
7	4.0	5.8	0.95	11.3			
8	4.6	4.8	1.1	9.3			
9	4.6	4.6	1.0	12.5			
10	4.95	6.1	0.36	9.6		3.55	
11	4.7	4.7	1.1	10.7			
12	4.1	4.3	1.0	11.3			
13	5.9	4.2	1.3	12.2			
14	5.05	6.3	0.37	10.0		1.08	
15	6.1	6.5	1.2	12.2			
16	4.1	5.0	1.0	11.3			
17	6.5	5.7	1.0	9.2			
19	4.6	6.2	1.1	8.8			
20	5.16	5.6	1.1	9.76	1.15		
21	5.18	4.78	1.1	9.61	0.61		
22	4.6	6.2	1.1	9.7			
23	4.7	5.0	1.0	8.9	0.60	0.44	0.41
25	5.10	6.3	1.1	9.64	1.72		

4.0 RESULTS AND DISCUSSION

Figure 4 shows the four basic surface morphologies observed on the specimens tested. Table 2 lists which of these morphologies dominated for each specimen tested. Morphology (c) indicates that the tested surface exhibited a rasiter pattern with dispersed cracks. These cracks were often faintly visible on the pretest polished specimen surface. Three alloy compositions (ID's 6,9,13) exhibited cracking. Table 1 indicates that the Al content in these three specimens was over 12.0 wt percent. The only specimen with more than 12.0 percent Al which did not crack was specimen 15. Of these four specimens, specimen 15 was the only alloy where the percentage of Fe exceeded the percentage Ni. The only alloy composition to exhibit a porous morphology (p) was 19 which had the lowest amount of Al content (8.8 percent). Specimens 32 and 33 exhibited smooth uniform wear. All the remaining specimens exhibited the rasiter wear pattern observed in previous studies [6].

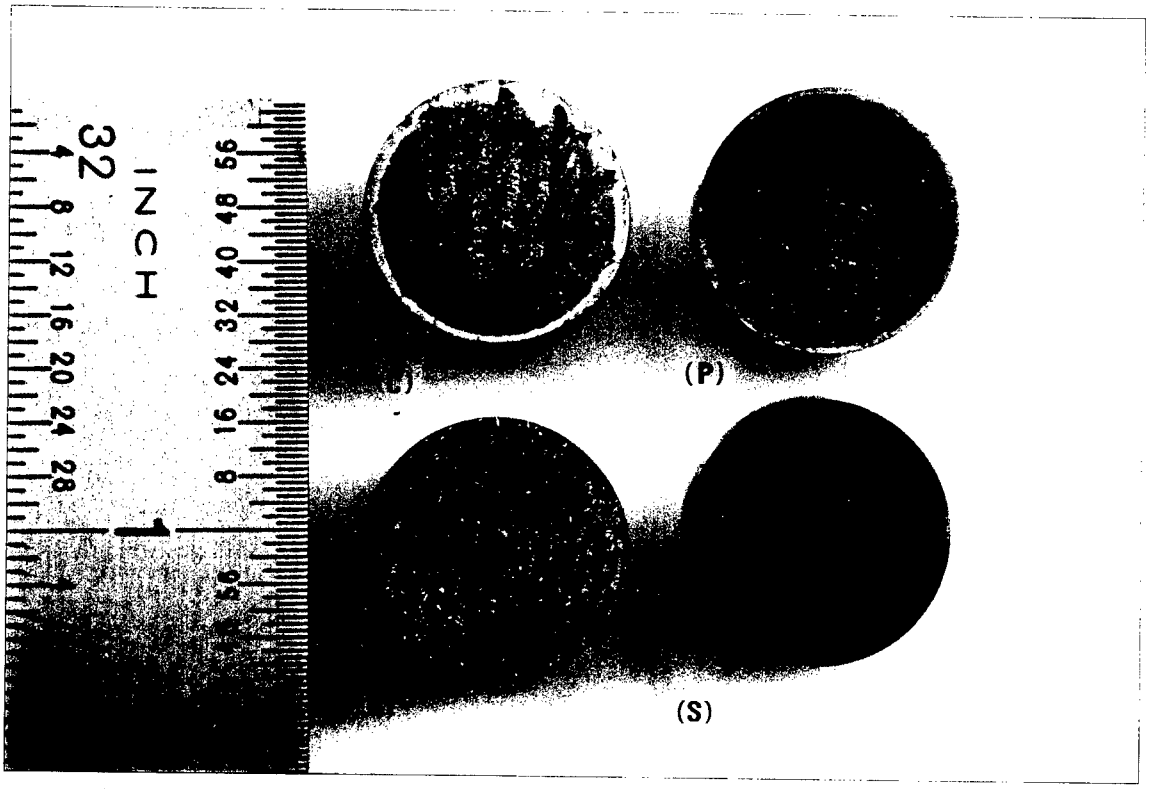

Figure 4 - Various specimen surface appearances observed subsequent to testing.

In general, the mean depth of penetration verses time relationships between duplicate specimens is reproducible. Table 2 and Figure 5 indicate that the overall erosion performance of an alloy depends on the amount of Al in the composition. All alloy compositions containing in excess of 10.7 percent of Al performed exceptionally well regardless of the visual appearance of the tested surface of the specimen (Figure 4). The only composition producing equivalent performance with less than 10.7 percent Al was specimen 25 which contained 9.64 percent Al and 1.72 percent Cr. The lowest performing alloys of the compositions listed in Table 1 were either low in AL (less than 9 percent) or contained additions of titanium (greater than 2 percent).

Table 2 - Summary of the cavitation results contained in Appendix B.

Specimen ID	Incub Time (hrs)	Max. Rate (um/hr)	Specimen ID	Incub Time (hrs)	Max. Rate (um/hr)	Avg Incub Time (hrs)	Rank	Avg Rate (um/hr)	Rank	Elapsed Time to 25 um (hrs)	Rank
1A(r/s)	1.01	2.53	1B(r/s)	1.14	2.35	1.075	22	2.44	21	11.3209	21
2A(r)	2.55	1.42	2B(r)	2.56	1.49	2.555	7	1.455	11	19.7371	10
3A(r)	1.77	1.97	3B(r)	1.44	1.97	1.605	17	1.97	19	14.2954	19
4A(r)	2.62	1.59	4B(r)	2.55	1.56	2.585	6	1.575	14	18.458	12
5A(r)	2.00	1.82	5B(r)	1.45	1.76	1.725	13	1.79	16	15.6915	16
6A(c)	3.32	1.21	6B(c)	3.25	1.09	3.285	2	1.15	6	25.0241	4
7A(r)	2.49	1.04	7B(r)	2.30	1.05	2.395	9	1.045	2	26.3184	3
8A(r)	1.83	2.04	8B(r)	1.91	1.79	1.87	12	1.915	17	14.9248	17
9A(c)	3.06	1.07	9B(c)	1.94	1.22	2.5	8	1.145	5	24.3341	6
10A(r)	n/t	n/t	10B								
11A(r)	2.01	1.13	11B(r)	2.06	1.09	2.035	10	1.11	4	24.5575	5
12A(r)	4.45	1.44	12B(r)	4.03	1.27	4.24	1	1.355	8	22.6902	7
13A(c)	2.53	1.01	13B(c)	3.80	1.11	3.165	3	1.06	3	26.7499	2
14A(r/s)	2.02	1.56	14B(r/s)	f/t	f/t	2.02	11	1.56	13	18.0456	14
15A(r)	2.64	0.98	15B(r)	3.09	0.99	2.865	4	0.985	1	28.2457	1
16A(r)	2.78	1.33	16B(r)	2.50	1.48	2.64	5	1.405	9	20.4336	9
17A(r)	1.40	1.93	17B(r)	1.78	1.94	1.59	18	1.935	18	14.5099	18
19A(p)	1.07	5.59	19B(p)	0.93	5.87	1	24	5.73	25	5.363	25
20A(r)	1.71	1.45	20B(r)	1.21	1.37	1.46	19	1.41	10	19.1905	11
21A(r)	1.71	1.46	21B(r)	1.71	1.59	1.71	14	1.525	12	18.1034	13
22A(r)	1.86	1.70	22B(r)	1.48	1.73	1.67	15	1.715	15	16.2473	15
23A(r/s)	1.17	2.70	23B(r/s)	1.20	2.60	1.185	21	2.65	22	10.619	22
25A(r)	1.67	1.31	25B(r)			1.67	16	1.31	7	20.754	8
30A(r)	1.24	2.14	30B(r)	f/t	f/t	1.24	20	2.14	20	12.9222	20
32A(s)	0.82	4.11	32B(s)	0.94	3.91	0.88	25	4.01	24	7.11441	24
33A(s)	0.93	3.54	33B(s)	1.09	3.40	1.01	23	3.47	23	8.2146	23

() letter in brackets refers to specimen surface morphology (see Figure 4).
n/t - indicates weight loss numbers were influenced by porosity in specimen.
f/t - indicates a fatigue crack formed in the specimen before enough useful data could be recorded.

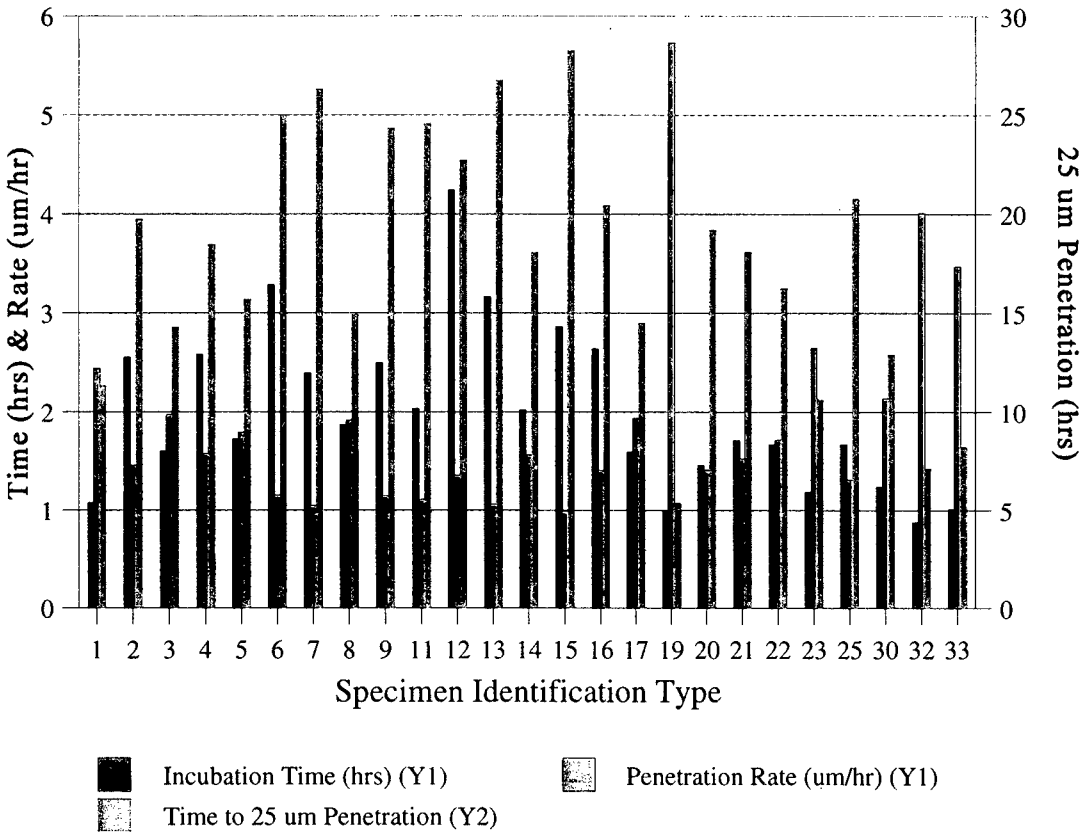

Figure 5 - Summary of average incubation time, penetration rate and time to 25 um penetration for the NAB chemistries tested.

For the alloys tested, it is observed that chemistries which produce above average overall performance (ie time to 25um penetration) generally have both above average incubation times and above average erosion rates. Several of the alloy compositions have exceptionally low erosion rates (low slope) when compared to the standards recommended in ASTM G-32. It is also observed in the graphs presented in Appendix B that for above average performers, the transition between incubation and sustained linear penetration is gradual. This expanded non-linear region may be a testing artifact associated with the engineered microstructural variation which exists across the surface of these specimens combined with the relatively low penetration rate. The low erosion rates observed tend to reduce the sensitivity of the linear extrapolation method used by ASTM G-32 to determine the incubation time. Thus while the generated incubation times may be reproducible between specimens, they may be non-conservative. This may in part account for the relatively high incubation times calculated for some of the alloy compositions.

5.0 CONCLUSIONS

The following inferences may be drawn from the data presented in this study:

- Alloy compositions tested with a minimum of 10.7 percent Al produced above average erosion performance.
- Additions of significant amounts of Cr to the alloy improved the erosion performance in alloy compositions with less than 10.7 percent Al.
- The alloy composition with 2.24 percent titanium degraded the erosion performance.
- The linear extrapolation method recommended in ASTM-G-32 for determining incubation times may generate non-conservative estimates owing to the expanded non-linear region observed for many of the specimens tested in this study.

6.0 REFERENCES

[1] C.V. Hyatt, C. Bennet, J. Gianetto and M. Sahoo, "Development of Microstructure in Laser Clad Nickel Aluminum Bronze", In preparation.

[2] C.V. Hyatt, K.H. Magee, J. Hewitt and T. Betancourt, "Laser Weld Cladding of Nickel Aluminum Bronzes", in Proceedings of the 2nd CF/CRAD Meeting on Naval Applications of Materials Technology, J.R. Matthews, ed., Halifax, N.S., May 2-4, 1995.

[3] C.V. Hyatt and K.H. Magee, "Laser Surface Melting and Cladding of Nickel Aluminum Bronzes", in Proceedings of Advanced Methods of Joining New Materials II, The American Welding Society, Miami, Florida, 1994, 111-126.

[4] J. Hewitt, V.E. Merchant, C. Hyatt and D.O. Morehouse, "Laser Beam Welding of Nickel Aluminum Bronze with a Fine Wire Feeder", In preparation.

[5] C.V. Hyatt, K. MacKay and T. Betancourt, "Evaluation of Laser Treated Copper Alloys", Materials Science and Technology, 250-254, 10, March 1994.

[6] Betancourt, T. "Cavitation Erosion Resistance of Laser-Treated Nickel Aluminum-Bronze", Final Report to DREA CR/94/458.

[7] Kapp, Daily and Hammit, Cavitation, McGraw-Hill, 1970, pp. 27.

[8] Hirotsu and Masato, "Cavitation Damage Mechanism and its Correlation to Physical Properties of Materials", Characterization and Determination of Erosion Resistance, ASTM STP474, 1970, pp.48.

APPENDIX A - Inconel Nickel 200 Apparatus Calibration Data

Sample Identification	Experimental Test Data			
	Elapsed Time (hrs)	Specimen Mass (g)	Cumulative Mass Loss (g)	Mean Depth of Erosion (μm)
System #1	0	11.8502	0.0000	0
	1	11.8030	0.0472	27.007368
	2	11.7437	0.1065	60.938235
	3	11.6826	0.1676	95.899044
	4	11.6251	0.2251	128.799969
	5	11.5869	0.2633	150.657627
	6	11.5537	0.2965	169.654335
	7	11.5272	0.3230	184.81737
	8	11.5029	0.3473	198.721587
System # 2	0	11.7646	0.0000	0
	1	11.7112	0.0534	30.554946
	2	11.6471	0.1175	67.232325
	3	11.5816	0.1830	104.71077
	4	11.5308	0.2338	133.778022
	5	11.4911	0.2735	156.493965
	6	11.4612	0.3034	173.602446
	7	11.4349	0.3297	188.651043
	8	11.4110	0.3536	202.326384

Table A.1 - Calibration specimen erosion data generated for the two ultrasonic converter assemblies used.

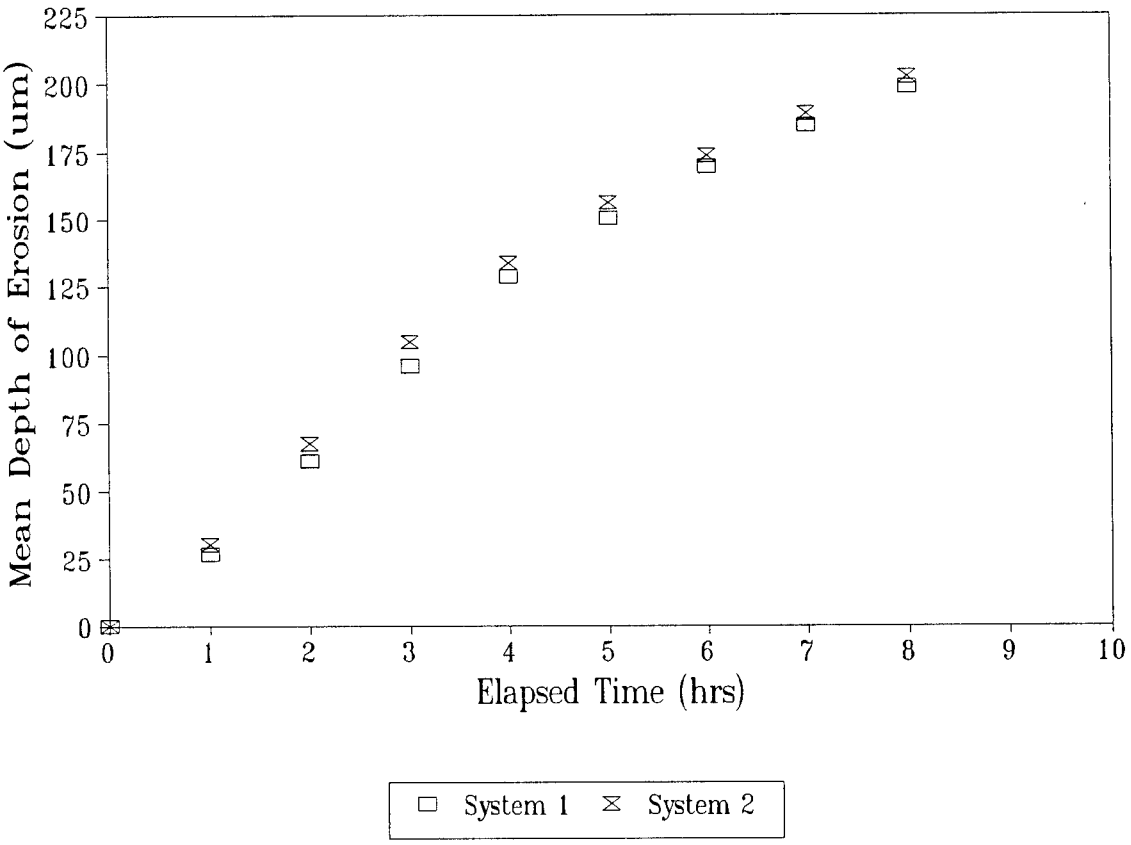

Figure A.1 - Inconel 200 calibration curves for the two systems.

APPENDIX B - Laser Surface Modified NAB Data

Sample Identification	Experimental Test Data			
	Elapsed Time (hrs)	Specimen Mass (g)	Cumulative Mass Loss (g)	Mean Depth of Erosion (μm)
1A	0	10.5957	0.0000	0
	1	10.5947	0.0010	0.6625324
	2	10.5919	0.0038	2.51762312
	3	10.5882	0.0075	4.968993
	4	10.5842	0.0115	7.6191226
	5	10.5807	0.0150	9.937986
	6	10.5770	0.0187	12.38935588
	7	10.5732	0.0225	14.906979
	8	10.5690	0.0267	17.68961508
	10	10.5604	0.0353	23.38739372
	11.82	10.5533	0.0424	28.09137376
	13.97	10.5460	0.0497	32.92786028
	16	10.5366	0.0591	39.15566484
1B	0	10.5338	0.0000	0
	1	10.5331	0.0007	0.46377268
	2	10.5307	0.0031	2.05385044
	3	10.5272	0.0066	4.37271384
	4	10.5236	0.0102	6.75783048
	5	10.5199	0.0139	9.20920036
	6	10.5169	0.0169	11.19679756
	7	10.5131	0.0207	13.71442068
	8.20	10.5085	0.0253	16.76206972
	10	10.5055	0.0283	18.74966692
	12	10.4947	0.0391	25.90501684
	14	10.4868	0.0470	31.1390228
	16	10.4797	0.0541	35.84300284

Table B.1 - Erosion data generated for specimens 1A and 1B

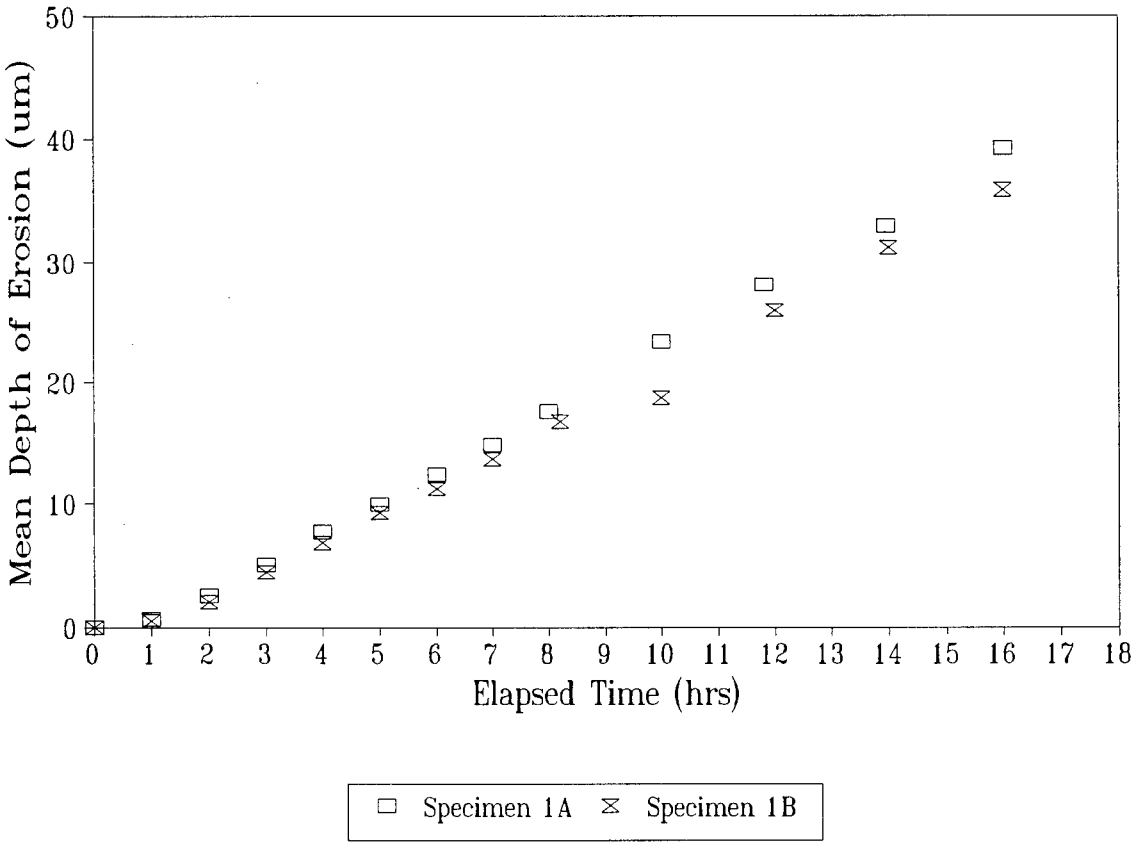

Figure B.1 - Erosion curves for specimens 1A and 1B.

Sample Identification	Experimental Test Data			
	Elapsed Time (hrs)	Specimen Mass (g)	Cumulative Mass Loss (g)	Mean Depth of Erosion (μm)
2A	0	10.6587	0.0000	0
	1	10.6587	0.0000	0
	2	10.6582	0.0005	0.3312662
	3	10.6568	0.0019	1.25881156
	4	10.6556	0.0031	2.05385044
	5	10.6532	0.0055	3.6439282
	6	10.6517	0.0070	4.6377268
	7	10.6489	0.0098	6.49281752
	8	10.6470	0.0117	7.75162908
	10	10.6429	0.0158	10.46801192
	12	10.6383	0.0204	13.51566096
	14	10.6347	0.0240	15.9007776
	16	10.6303	0.0284	18.81592016
2B	0	10.6268	0.0000	0
	1	10.6261	0.0007	0.46377268
	2	10.6259	0.0009	0.59627916
	3.03	10.6249	0.0019	1.25881156
	4	10.6234	0.0034	2.25261016
	5	10.6212	0.0056	3.71018144
	6	10.6188	0.0080	5.3002592
	7	10.6168	0.0100	6.625324
	8	10.6149	0.0119	7.88413556
	10	10.6106	0.0162	10.73302488
	12	10.6049	0.0219	14.50945956
	14	10.6008	0.0260	17.2258424
	16	10.5964	0.0304	20.14098496

Table B.2 - Erosion data generated for specimens 2A and 2B

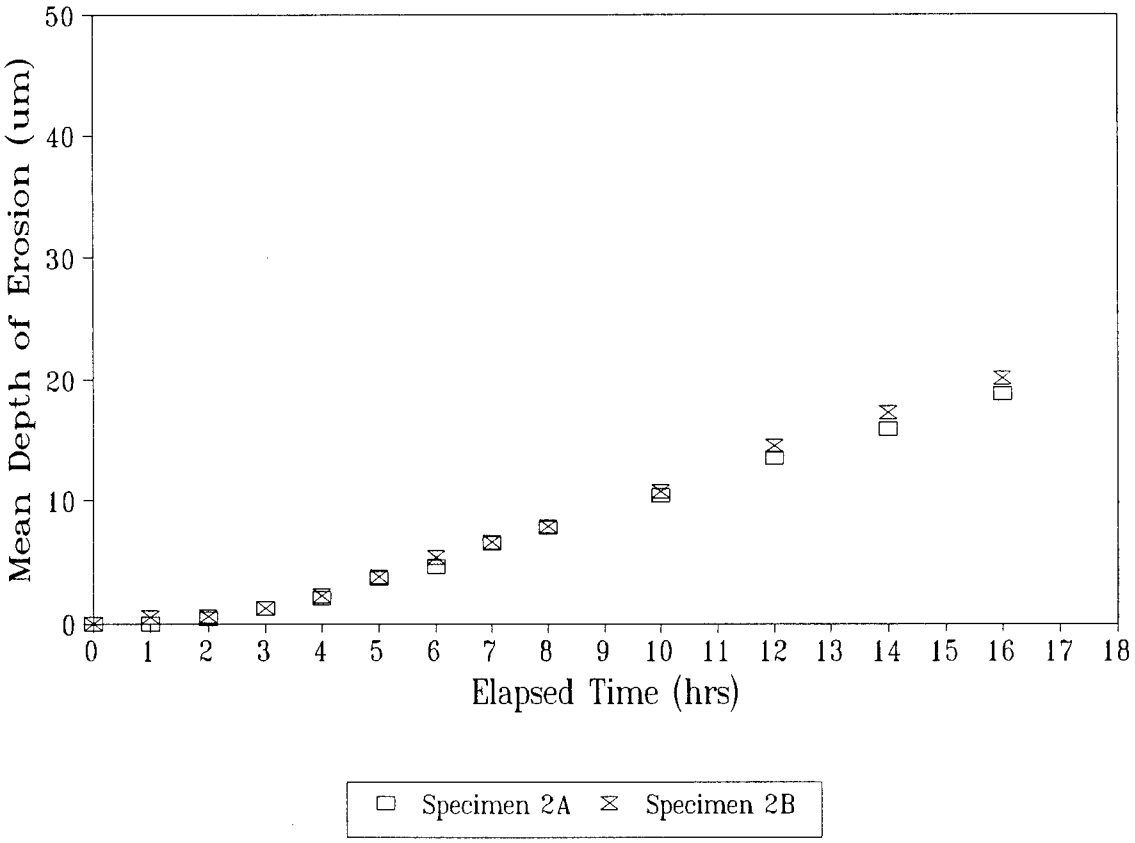

Figure B.2 - Erosion curves for specimens 2A and 2B

Sample Identification	Experimental Test Data			
	Elapsed Time (hrs)	Specimen Mass (g)	Cumulative Mass Loss (g)	Mean Depth of Erosion (μm)
3A	0	10.8126	0.0000	0
	1	10.8124	0.0002	0.13250648
	2	10.8112	0.0014	0.92754536
	3	10.8088	0.0038	2.51762312
	4	10.8059	0.0067	4.43896708
	5	10.8034	0.0092	6.09529808
	6	10.7998	0.0128	8.48041472
	7	10.7972	0.0154	10.20299896
	8.17	10.7933	0.0193	12.78687532
	10	10.7881	0.0245	16.2320438
	12	10.7822	0.0304	20.14098496
	14	10.7762	0.0364	24.11617936
	16	10.7704	0.0422	27.95886728
3B	0	10.8145	0.0000	0
	1	10.8139	0.0006	0.39751944
	2	10.8119	0.0026	1.72258424
	3	10.8094	0.0051	3.37891524
	4	10.8066	0.0079	5.23400596
	5	10.8041	0.0104	6.89033696
	6	10.8012	0.0133	8.81168092
	7	10.7980	0.0165	10.9317846
	8	10.7954	0.0191	12.65436884
	10	10.7889	0.0256	16.96082944
	12	10.7826	0.0319	21.13478356
	14	10.7773	0.0372	24.64620528
	16	10.7713	0.0432	28.62139968

Table B.3 - Erosion data generated for specimens 3A and 3B

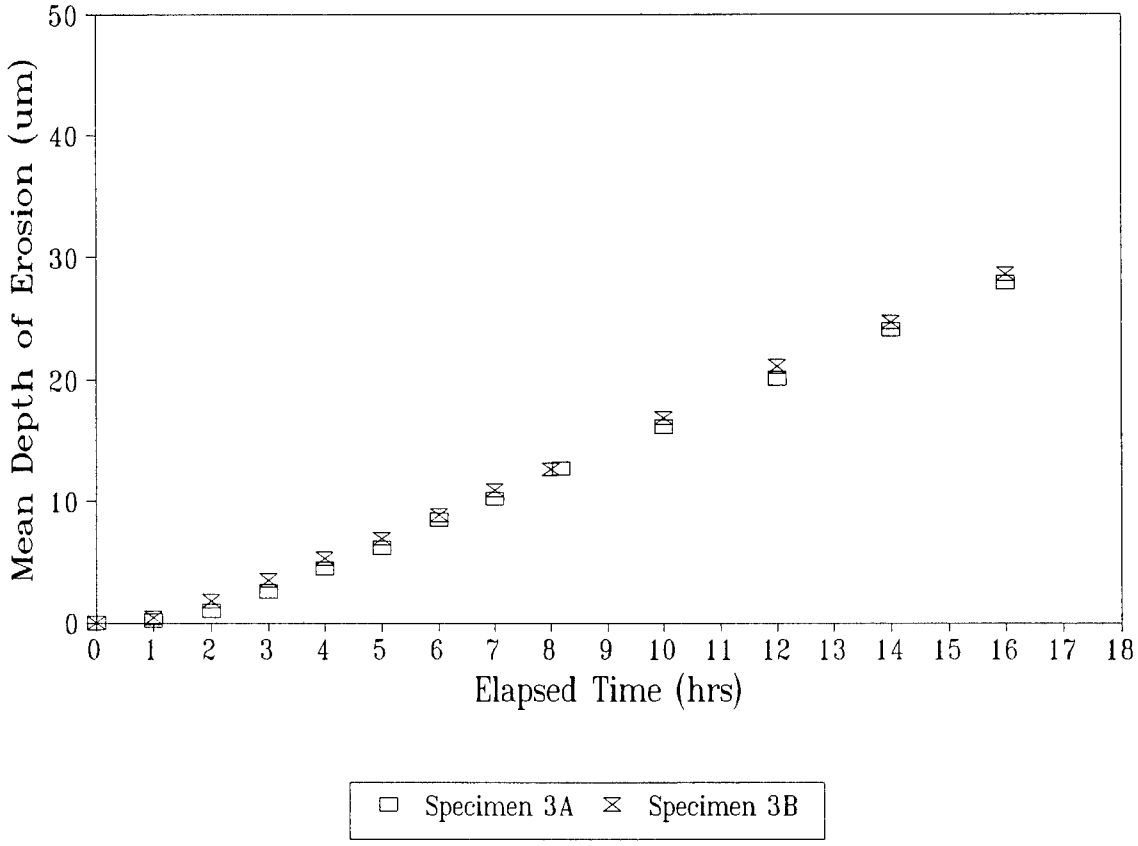

Figure B.3 - Erosion curves for specimens 3A and 3B

Sample Identification	Experimental Test Data			
	Elapsed Time (hrs)	Specimen Mass (g)	Cumulative Mass Loss (g)	Mean Depth of Erosion (μm)
4A	0	10.6854	0.0000	0
	1	10.6846	0.0008	0.53002592
	2	10.6842	0.0012	0.79503888
	3	10.6831	0.0023	1.52382452
	4	10.6816	0.0038	2.51762312
	5	10.6796	0.0058	3.84268792
	6	10.6776	0.0078	5.16775272
	7	10.6752	0.0102	6.75783048
	8	10.6726	0.0128	8.48041472
	10	10.6676	0.0178	11.79307672
	12	10.6625	0.0229	15.17199196
	14	10.6576	0.0278	18.41840072
	16	10.6522	0.0332	21.99607568
4B	0	10.7035	0.0000	0
	1	10.7028	0.0007	0.46377268
	2	10.7026	0.0009	0.59627916
	3	10.7014	0.0021	1.39131804
	4	10.6997	0.0038	2.51762312
	5	10.6974	0.0061	4.04144764
	6	10.6956	0.0079	5.23400596
	7	10.6932	0.0103	6.82408372
	8	10.6912	0.0123	8.14914852
	10	10.6859	0.0176	11.66057024
	12	10.6808	0.0227	15.03948548
	14	10.6755	0.0280	18.5509072
	16	10.6704	0.0331	21.92982244

Table B.4 - Erosion data generated for specimens 4A and 4B

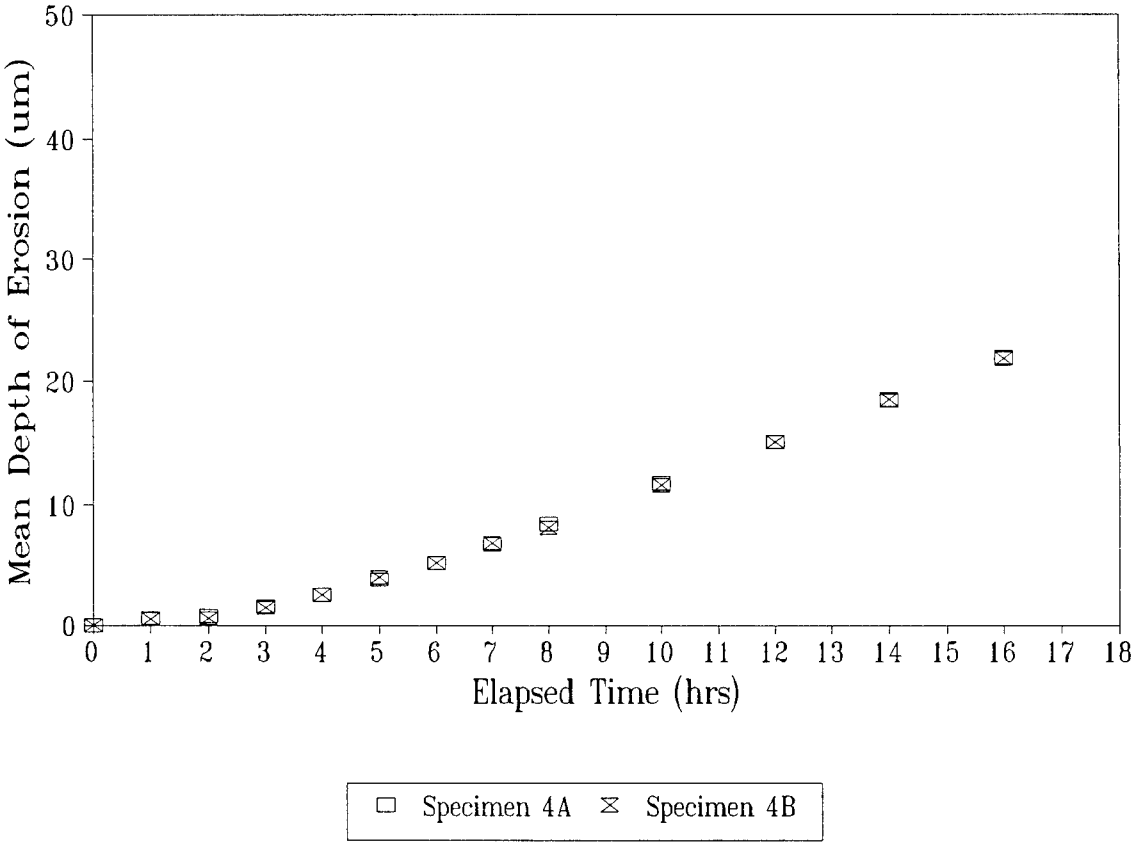

Figure B.4 - Erosion curves for specimens 4A and 4B

Sample Identification	Experimental Test Data			
	Elapsed Time (hrs)	Specimen Mass (g)	Cumulative Mass Loss (g)	Mean Depth of Erosion (μm)
5A	0	10.8432	0.0000	0
	1	10.8428	0.0004	0.26501296
	2	10.8420	0.0012	0.79503888
	3	10.8401	0.0031	2.05385044
	4	10.8380	0.0052	3.44516848
	5	10.8351	0.0081	5.36651244
	6	10.8323	0.0109	7.22160316
	7	10.8294	0.0138	9.14294712
	8	10.8266	0.0166	10.99803784
	10	10.8212	0.0220	14.5757128
	12.32	10.8144	0.0288	19.08093312
	14	10.8100	0.0332	21.99607568
	16	10.8046	0.0386	25.57375064
5B	0	10.8316	0.0000	0
	1.48	10.8306	0.0010	0.6625324
	2	10.8294	0.0022	1.45757128
	3	10.8273	0.0043	2.84888932
	4	10.8246	0.0070	4.6377268
	5	10.8221	0.0095	6.2940578
	6	10.8196	0.0120	7.9503888
	7	10.8170	0.0146	9.67297304
	8	10.8147	0.0169	11.19679756
	10	10.8083	0.0233	15.43700492
	13	10.7993	0.0323	21.39979652
	14	10.7964	0.0352	23.32114048
	16	10.7912	0.0404	26.76630896

Table B.5 - Erosion data generated for specimens 5A and 5B

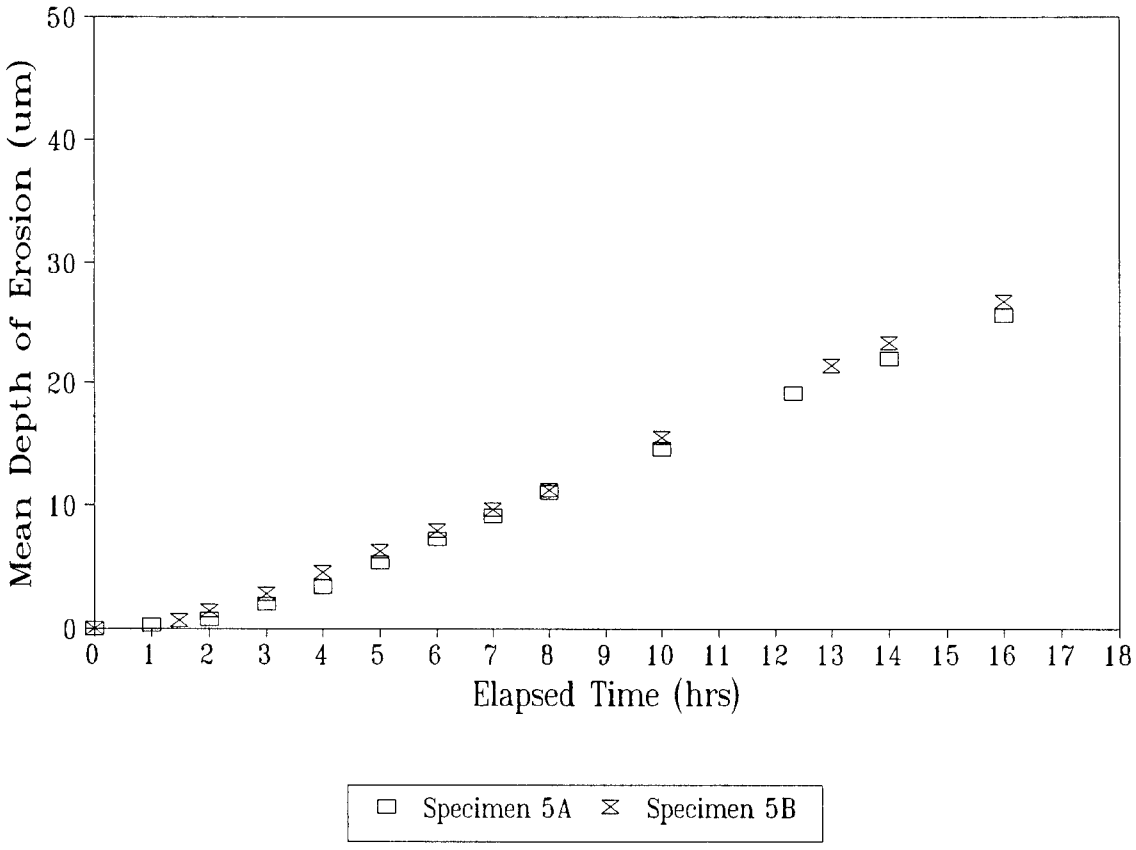

Figure B.5 - Erosion curves for specimens 5A and 5B

Sample Identification	Experimental Test Data			
	Elapsed Time (hrs)	Specimen Mass (g)	Cumulative Mass Loss (g)	Mean Depth of Erosion (μm)
6A	0	10.3194	0.0000	0
	1	10.3192	0.0002	0.13250648
	2	10.3186	0.0008	0.53002592
	3	10.3179	0.0015	0.9937986
	4	10.3169	0.0025	1.656331
	5	10.3160	0.0034	2.25261016
	6	10.3142	0.0052	3.44516848
	7	10.3131	0.0063	4.17395412
	8	10.3109	0.0085	5.6315254
	10	10.3074	0.0120	7.9503888
	12	10.3037	0.0157	10.40175868
	14	10.2995	0.0199	13.18439476
	16	10.2962	0.0232	15.37075168
6B	0	10.3231	0.0000	0
	1	10.3227	0.0004	0.26501296
	2	10.3217	0.0014	0.92754536
	3	10.3215	0.0016	1.06005184
	4.45	10.3207	0.0024	1.59007776
	5	10.3194	0.0037	2.45136988
	6	10.3186	0.0045	2.9813958
	7	10.3173	0.0058	3.84268792
	8	10.3157	0.0074	4.90273976
	10	10.3124	0.0107	7.08909668
	12	10.3086	0.0145	9.6067198
	14	10.3051	0.0180	11.9255832
	16	10.3004	0.0227	15.03948548

Table B.6 - Erosion data generated for specimens 6A and 6B

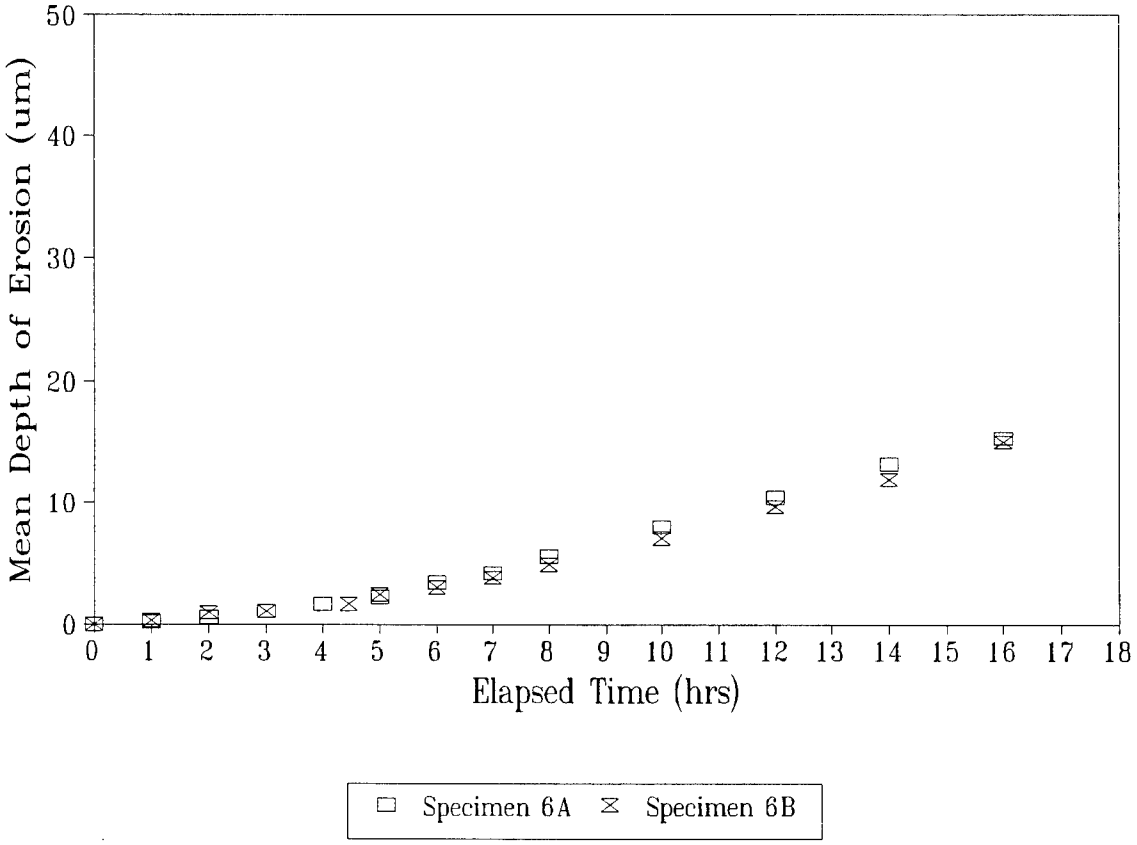

Figure B.6 - Erosion curves for specimens 6A and 6B

Sample Identification	Experimental Test Data			
	Elapsed Time (hrs)	Specimen Mass (g)	Cumulative Mass Loss (g)	Mean Depth of Erosion (μm)
7A	0	10.5419	0.0000	0
	1	10.5416	0.0003	0.19875972
	2	10.5408	0.0011	0.72878564
	3	10.5400	0.0019	1.25881156
	4	10.5391	0.0028	1.85509072
	5	10.5378	0.0041	2.71638284
	6	10.5363	0.0056	3.71018144
	7	10.5350	0.0069	4.57147356
	8	10.5334	0.0085	5.6315254
	10	10.5306	0.0113	7.48661612
	12	10.5268	0.0151	10.00423924
	14	10.5233	0.0186	12.32310264
	16	10.5197	0.0222	14.70821928
7B	0	10.5184	0.0000	0
	1	10.5178	0.0006	0.39751944
	2	10.5173	0.0011	0.72878564
	3	10.5160	0.0024	1.59007776
	4	10.5152	0.0032	2.12010368
	5	10.5140	0.0044	2.91514256
	6	10.5127	0.0057	3.77643468
	7	10.5112	0.0072	4.77023328
	8	10.5093	0.0091	6.02904484
	10	10.5063	0.0121	8.01664204
	12	10.5031	0.0153	10.13674572
	14.27	10.4993	0.0191	12.65436884
	16	10.4956	0.0228	15.10573872

Table B.7 - Erosion data generated for specimens 7A and 7B

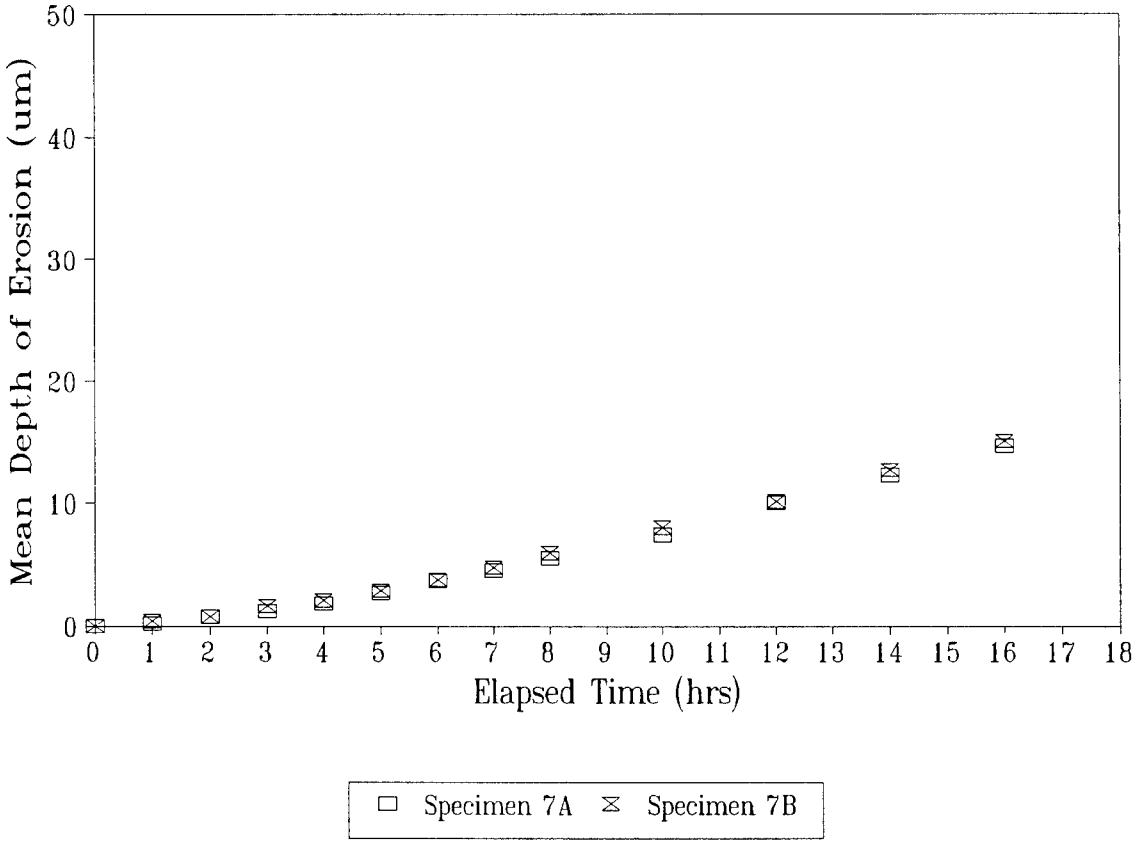

Figure B.7 - Erosion curves for specimens 7A and 7B.

Sample Identification	Experimental Test Data			
	Elapsed Time (hrs)	Specimen Mass (g)	Cumulative Mass Loss (g)	Mean Depth of Erosion (μm)
8A	0	10.8804	0.0000	0
	1	10.8801	0.0003	0.19875972
	2	10.8785	0.0019	1.25881156
	3	10.8764	0.0040	2.6501296
	4	10.8737	0.0067	4.43896708
	5	10.8704	0.0100	6.625324
	6	10.8677	0.0127	8.41416148
	7	10.8647	0.0157	10.40175868
	8	10.8620	0.0184	12.19059616
	10	10.8553	0.0251	16.62956324
	12	10.8485	0.0319	21.13478356
	14	10.8428	0.0376	24.91121824
	16	10.8366	0.0438	29.01891912
8B	0	10.8545	0.0000	0
	1	10.8541	0.0004	0.26501296
	2	10.8529	0.0016	1.06005184
	3	10.8515	0.0030	1.9875972
	4	10.8487	0.0058	3.84268792
	5	10.8463	0.0082	5.43276568
	6	10.8437	0.0108	7.15534992
	7	10.8407	0.0138	9.14294712
	8	10.8379	0.0166	10.99803784
	10	10.8327	0.0218	14.44320632
	12	10.8272	0.0273	18.08713452
	14	10.8197	0.0348	23.05612752
	16	10.8157	0.0388	25.70625712

Table B.8 - Erosion data generated for specimens 8A and 8B

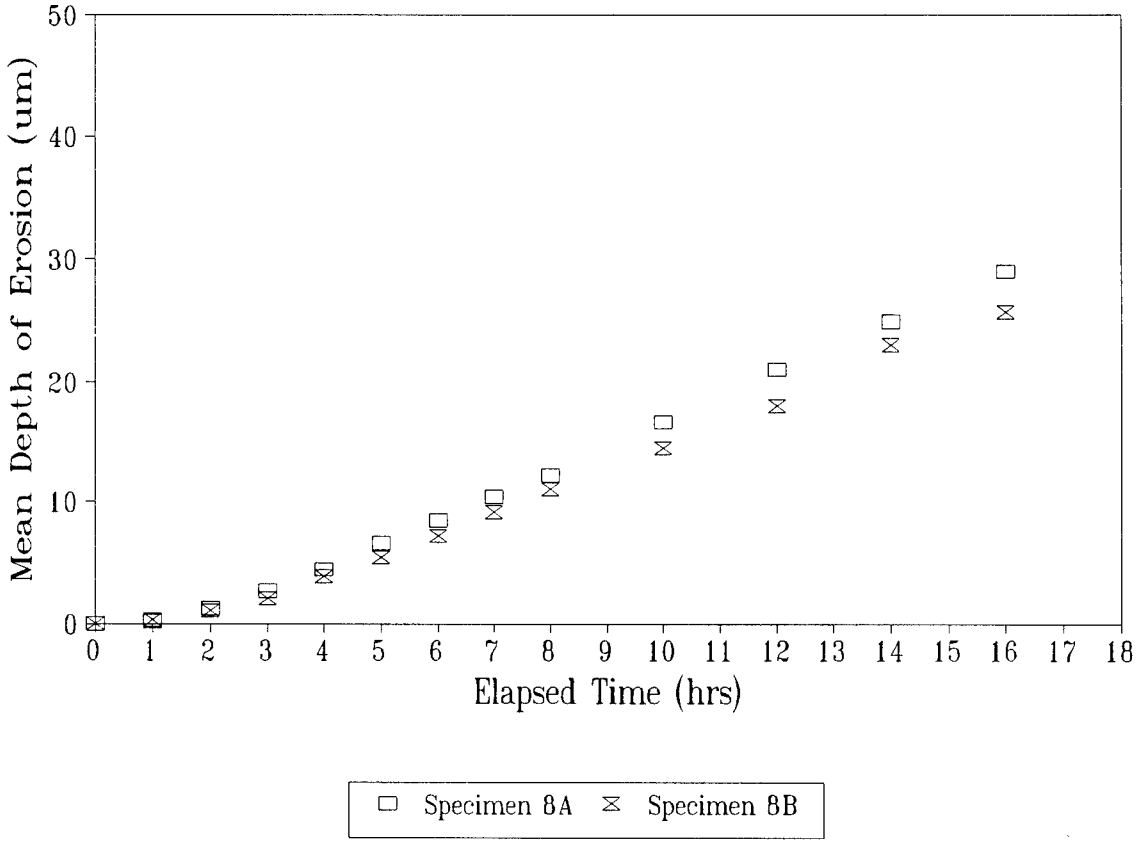

Figure B.8 - Erosion curves for specimens 8A and 8B.

Sample Identification	Experimental Test Data			
	Elapsed Time (hrs)	Specimen Mass (g)	Cumulative Mass Loss (g)	Mean Depth of Erosion (μm)
9A	0	10.2438	0.0000	0
	1	10.2433	0.0005	0.3312662
	2	10.2428	0.0010	0.6625324
	3	10.2421	0.0017	1.12630508
	4	10.2414	0.0024	1.59007776
	5	10.2402	0.0036	2.38511664
	6	10.2391	0.0047	3.11390228
	7	10.2379	0.0059	3.90894116
	8	10.2356	0.0082	5.43276568
	10	10.2328	0.0110	7.2878564
	12	10.2291	0.0147	9.73922628
	14	10.2260	0.0178	11.79307672
	16	10.2227	0.0211	13.97943364
9B	0	10.2155	0.0000	0
	1	10.2152	0.0003	0.19875972
	2	10.2147	0.0008	0.53002592
	3	10.2139	0.0016	1.06005184
	4.33	10.2114	0.0041	2.71638284
	5	10.2100	0.0055	3.6439282
	6	10.2080	0.0075	4.968993
	7	10.2061	0.0094	6.22780456
	8	10.2043	0.0112	7.42036288
	10	10.2004	0.0151	10.00423924
	12	10.1971	0.0184	12.19059616
	14	10.1933	0.0222	14.70821928
	16	10.1898	0.0257	17.02708268

Table B.9 - Erosion data generated for specimens 9A and 9B

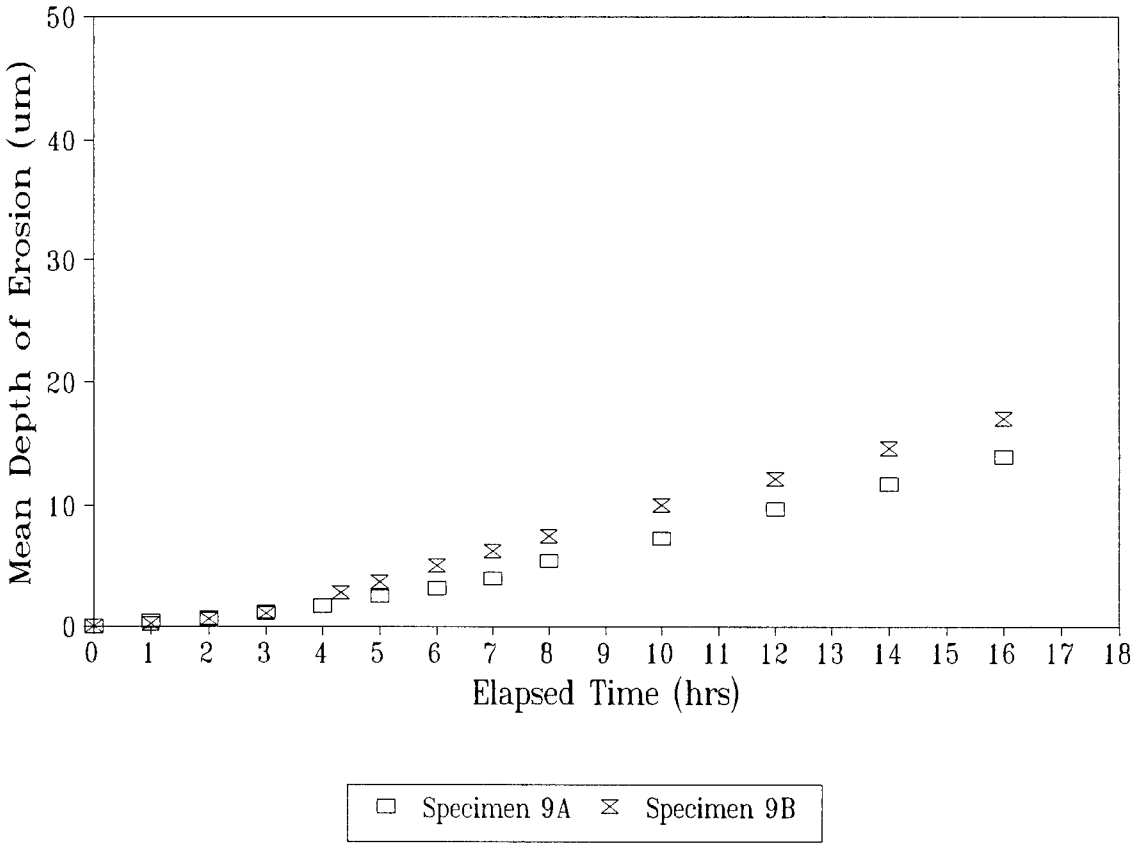

Figure B.9 - Erosion curves for specimens 9A and 9B.

Sample Identification	Experimental Test Data			
	Elapsed Time (hrs)	Specimen Mass (g)	Cumulative Mass Loss (g)	Mean Depth of Erosion (μm)
10 A	0	10.5426	0.0000	0
	1	10.5477	-0.0051	-3.37891524
	2	10.5471	-0.0045	-2.9813958
	3	10.5422	0.0004	0.26501296
	4	10.5396	0.0030	1.9875972
	5	10.5353	0.0073	4.83648652
	6	10.5322	0.0104	6.89033696
Discontinued	7	10.4812	0.0614	40.67948936
owing to	8			
loss of	10			
threads	12			
(porosity)	14			
	16			
10B	0			
Not tested	1			
owing to	2			
porosity	3			
	4			
	5			
	6			
	7			
	8			
	10			
	12			
	14			
	16			

Table B.10 - Erosion data generated for specimens 10A and 10B

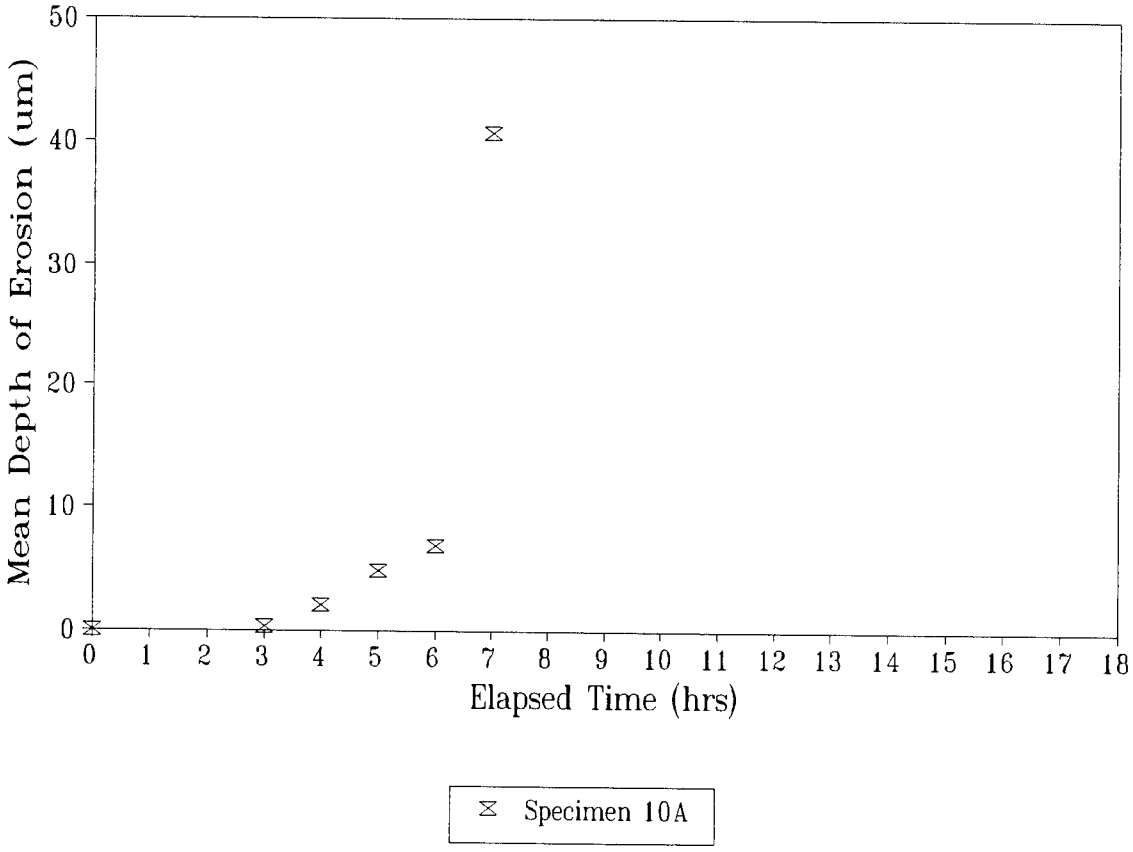

Figure B.10 - Erosion curve for specimen 10A.

Sample Identification	Experimental Test Data			
	Elapsed Time (hrs)	Specimen Mass (g)	Cumulative Mass Loss (g)	Mean Depth of Erosion (μm)
11A	0	10.5727	0.0000	0
	1	10.5722	0.0005	0.3312662
	2	10.5716	0.0011	0.72878564
	3	10.5702	0.0025	1.656331
	4	10.5694	0.0033	2.18635692
	5	10.5677	0.0050	3.312662
	6	10.5665	0.0062	4.10770088
	7	10.5645	0.0082	5.43276568
	8	10.5626	0.0101	6.69157724
	10	10.5586	0.0141	9.34170684
	12	10.5556	0.0171	11.32930404
	14	10.5517	0.0210	13.9131804
	16	10.5481	0.0246	16.29829704
11B	0	10.5766	0.0000	0
	1	10.5762	0.0004	0.26501296
	2	10.5761	0.0005	0.3312662
	3	10.5748	0.0018	1.19255832
	4	10.5732	0.0034	2.25261016
	5	10.5719	0.0047	3.11390228
	6	10.5704	0.0062	4.10770088
	7	10.5686	0.0080	5.3002592
	8	10.5669	0.0097	6.42656428
	10	10.5635	0.0131	8.67917444
	12	10.5600	0.0166	10.99803784
	14	10.5567	0.0199	13.18439476
	16	10.5533	0.0233	15.43700492

Table B.11 - Erosion data generated for specimens 11A and 11B

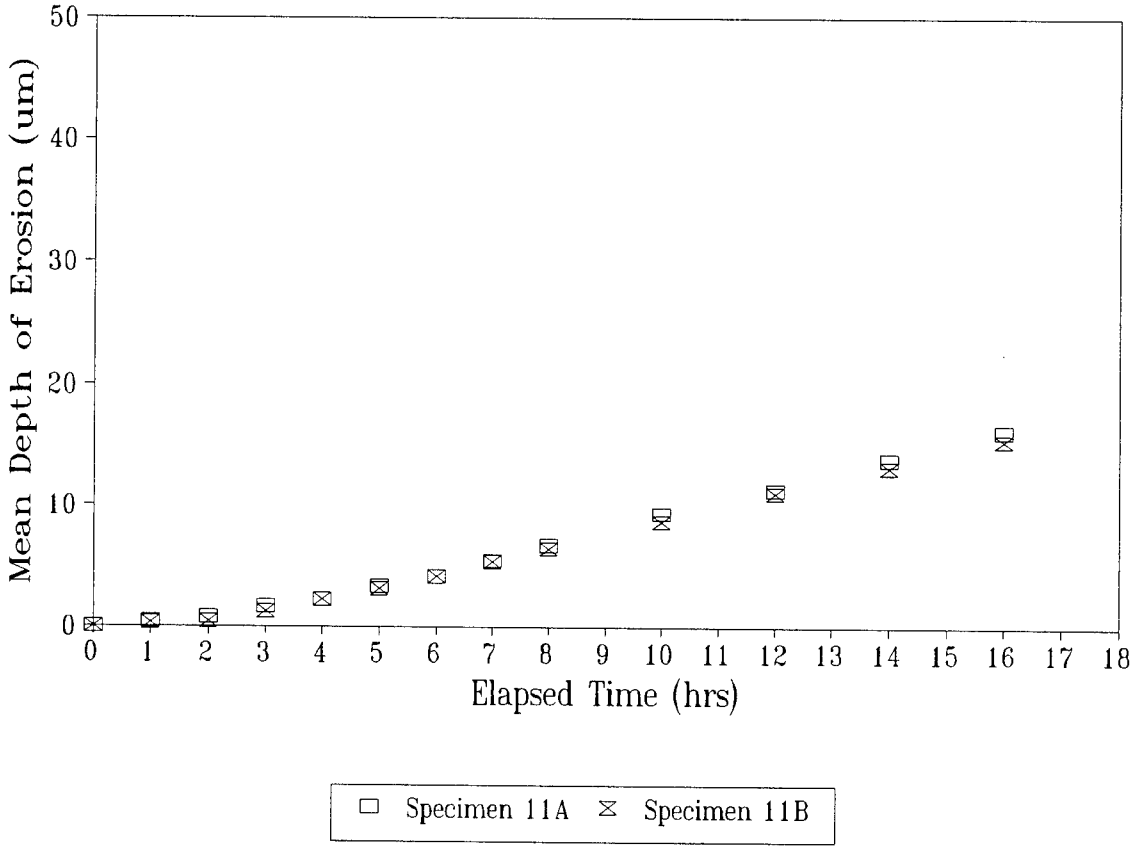

Figure B.11 - Erosion curves for specimens 11A and 11B.

Sample Identification	Experimental Test Data			
	Elapsed Time (hrs)	Specimen Mass (g)	Cumulative Mass Loss (g)	Mean Depth of Erosion (μm)
12A	0	10.4794	0.0000	0
	1	10.4790	0.0004	0.26501296
	2	10.4785	0.0009	0.59627916
	3	10.4781	0.0013	0.86129212
	4	10.4777	0.0017	1.12630508
	5	10.4764	0.0030	1.9875972
	6	10.4755	0.0039	2.58387636
	7	10.4738	0.0056	3.71018144
	8	10.4720	0.0074	4.90273976
	10	10.4680	0.0114	7.55286936
	12	10.4630	0.0164	10.86553136
	14	10.4583	0.0211	13.97943364
	16	10.4536	0.0258	17.09333592
12B	0	10.4766	0.0000	0
	1	10.4762	0.0004	0.26501296
	2	10.4758	0.0008	0.53002592
	3	10.4751	0.0015	0.9937986
	4	10.4740	0.0024	1.59007776
	5	10.4730	0.0034	2.25261016
	6	10.4722	0.0044	2.91514256
	7	10.4707	0.0059	3.90894116
	8.23	10.4690	0.0076	5.03524624
	10.23	10.4653	0.0113	7.48661612
	12	10.4615	0.0151	10.00423924
	14	10.4569	0.0197	13.05188828
	16	10.4517	0.0249	16.49705676

Table B.12 - Erosion data generated for specimens 12A and 12B

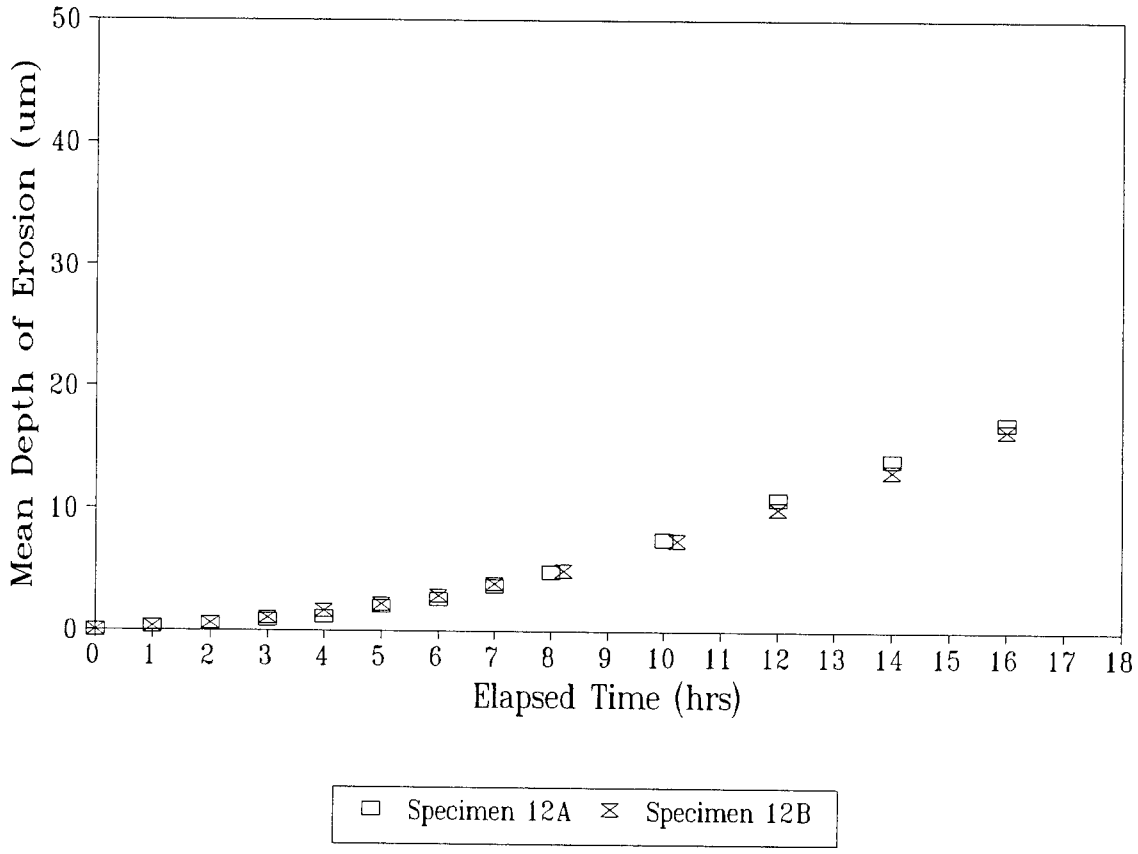

Figure B.12 - Erosion curves for specimens 12A and 12B.

Sample Identification	Experimental Test Data			
	Elapsed Time (hrs)	Specimen Mass (g)	Cumulative Mass Loss (g)	Mean Depth of Erosion (μm)
13A	0	10.2896	0.0000	0
	1	10.2891	0.0005	0.3312662
	2	10.2887	0.0009	0.59627916
	3	10.2877	0.0019	1.25881156
	4	10.2870	0.0026	1.72258424
	5	10.2857	0.0039	2.58387636
	6	10.2842	0.0054	3.57767496
	7	10.2829	0.0067	4.43896708
	8	10.2811	0.0085	5.6315254
	10	10.2780	0.0116	7.68537584
	12	10.2753	0.0143	9.47421332
	14	10.2722	0.0174	11.52806376
	16	10.2686	0.0210	13.9131804
	18	10.2656	0.0240	15.9007776
	20	10.2623	0.0273	18.08713452
13B	0	10.2914	0.0000	0
	1	10.2908	0.0006	0.39751944
	2	10.2906	0.0008	0.53002592
	3	10.2904	0.0010	0.6625324
	4	10.2900	0.0014	0.92754536
	5	10.2888	0.0026	1.72258424
	6	10.2874	0.0040	2.6501296
	7	10.2861	0.0053	3.51142172
	8	10.2850	0.0064	4.24020736
	10	10.2813	0.0101	6.69157724
	12	10.2778	0.0136	9.01044064
	14	10.2742	0.0172	11.39555728
	16	10.2705	0.0209	13.84692716

Table B.13 - Erosion data generated for specimens 13A and 13B

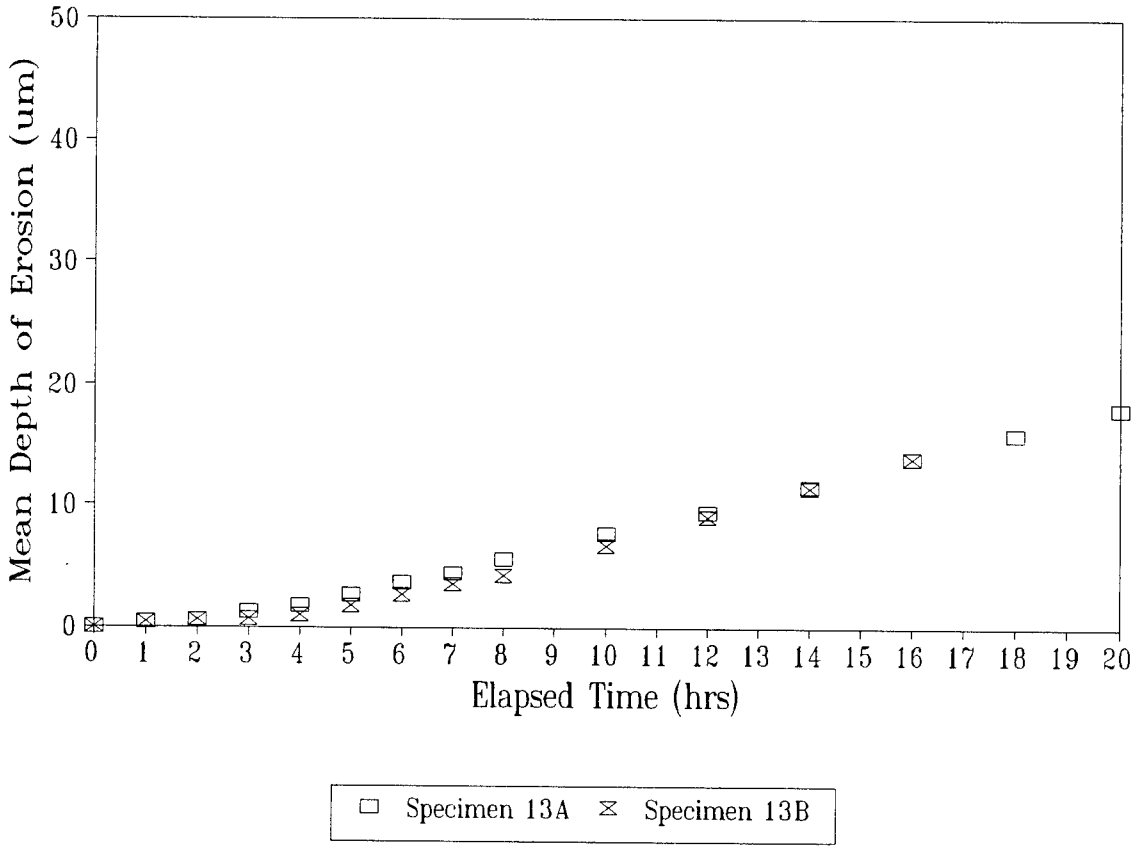

Figure B.13 - Erosion curves for specimens 13A and 13B.

Sample Identification	Experimental Test Data			
	Elapsed Time (hrs)	Specimen Mass (g)	Cumulative Mass Loss (g)	Mean Depth of Erosion (μm)
14A	0	10.7094	0.0000	0
	1	10.7091	0.0003	0.19875972
	2	10.7085	0.0009	0.59627916
	3	10.7065	0.0029	1.92134396
	4	10.7047	0.0047	3.11390228
	5	10.7026	0.0068	4.50522032
	6	10.7002	0.0092	6.09529808
	7	10.6977	0.0117	7.75162908
	8	10.6956	0.0138	9.14294712
	10	10.6904	0.0190	12.5881156
	12	10.6855	0.0239	15.83452436
	14	10.6810	0.0284	18.81592016
	16	10.6761	0.0333	22.06232892
14B	0	10.7289	0.0000	0
	1	10.7284	0.0005	0.3312662
	2	10.7272	0.0017	1.12630508
	3	10.7255	0.0034	2.25261016
Test Aborted lost thread	4	10.6593	0.0696	46.11225504
	5			
	6			
	7			
	8			
	10			
	12			
	14			
	16			

Table B.14 - Erosion data generated for specimens 14A and 14B

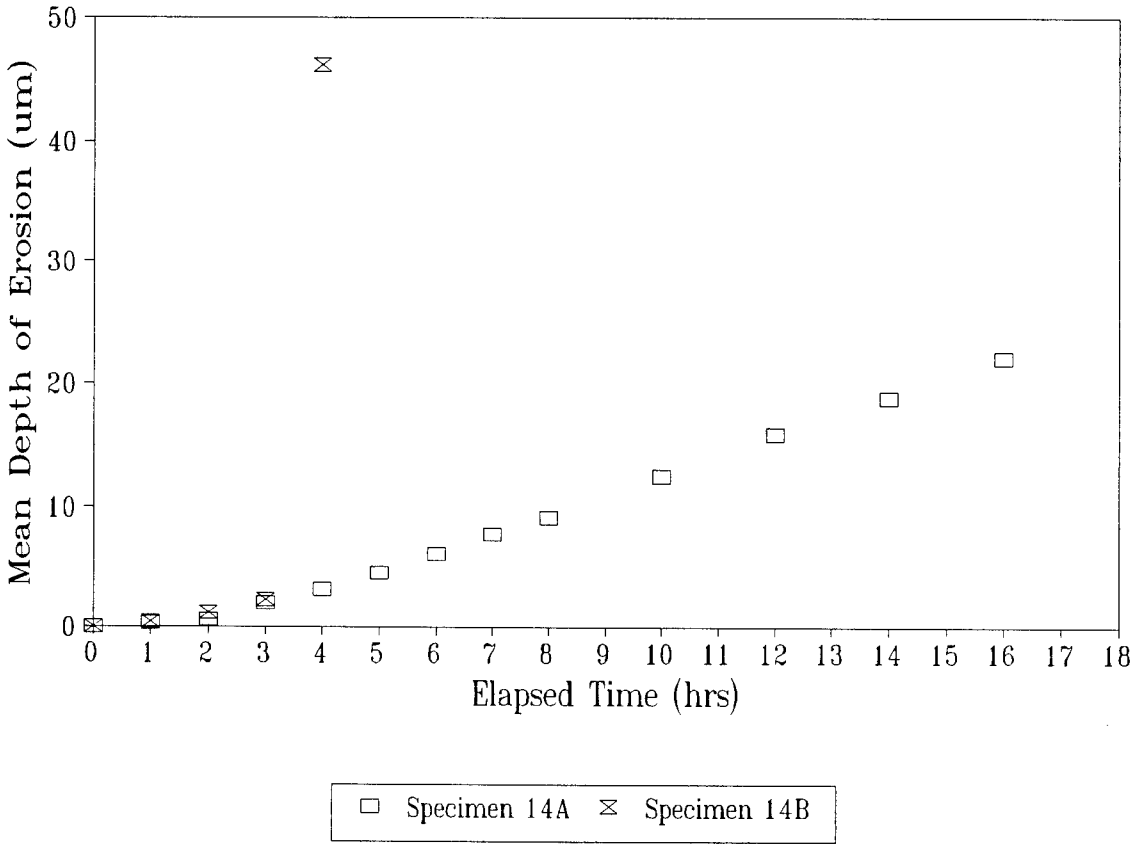

Figure B.14 - Erosion curves for specimens 14A and 14B.

Sample Identification	Experimental Test Data			
	Elapsed Time (hrs)	Specimen Mass (g)	Cumulative Mass Loss (g)	Mean Depth of Erosion (μm)
15A	0	10.4452	0.0000	0
	1	10.4448	0.0004	0.26501296
	2	10.4446	0.0006	0.39751944
	3	10.4437	0.0015	0.9937986
	4	10.4427	0.0025	1.656331
	5	10.4413	0.0039	2.58387636
	6	10.4402	0.0050	3.312662
	7	10.4388	0.0064	4.24020736
	8	10.4377	0.0075	4.968993
	10	10.4347	0.0105	6.9565902
	12	10.4316	0.0136	9.01044064
	14	10.4284	0.0168	11.13054432
	16	10.4254	0.0198	13.11814152
15B	0	10.4549	0.0000	0
	1	10.4547	0.0002	0.13250648
	2	10.4538	0.0011	0.72878564
	3	10.4535	0.0014	0.92754536
	4	10.4528	0.0021	1.39131804
	5	10.4517	0.0032	2.12010368
	6	10.4505	0.0044	2.91514256
	7.07	10.4490	0.0059	3.90894116
	8	10.4478	0.0071	4.70398004
	10	10.4450	0.0099	6.55907076
	12	10.4421	0.0128	8.48041472
	14	10.4386	0.0163	10.79927812
	16	10.4355	0.0194	12.85312856

Table B.15 - Erosion data generated for specimens 15A and 15B

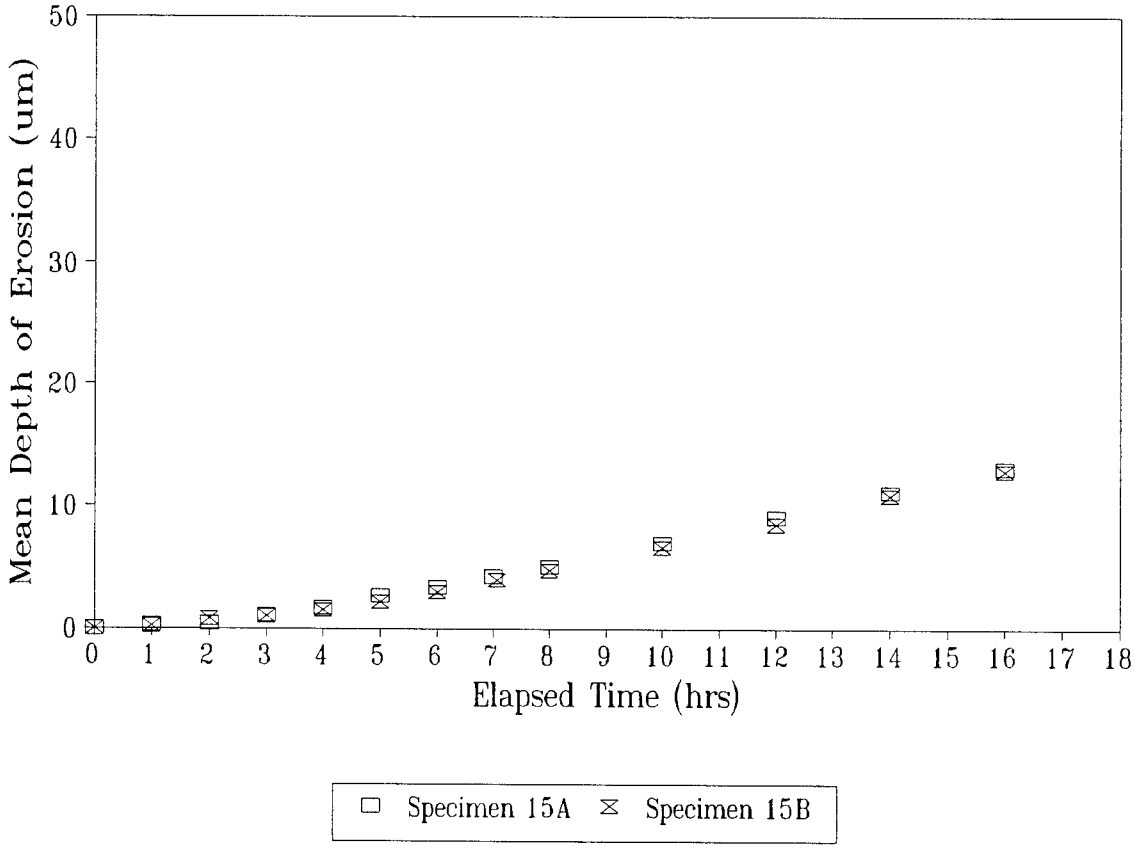

Figure B.15 - Erosion curves for specimens 15A and 15B.

Sample Identification	Experimental Test Data			
	Elapsed Time (hrs)	Specimen Mass (g)	Cumulative Mass Loss (g)	Mean Depth of Erosion (μm)
16A	0	10.5560	0.0000	0
	1	10.5557	0.0003	0.19875972
	2	10.5552	0.0008	0.53002592
	3	10.5543	0.0017	1.12630508
	4	10.5531	0.0029	1.92134396
	5	10.5516	0.0044	2.91514256
	6	10.5496	0.0064	4.24020736
	7.1	10.5476	0.0084	5.56527216
	8	10.5457	0.0103	6.82408372
	10	10.5414	0.0146	9.67297304
	12	10.5372	0.0188	12.45560912
	14	10.5325	0.0235	15.5695114
	16	10.5282	0.0278	18.41840072
16B	0	10.5715	0.0000	0
	1	10.5711	0.0004	0.26501296
	2	10.5707	0.0008	0.53002592
	3	10.5699	0.0016	1.06005184
	4	10.5677	0.0038	2.51762312
	5	10.5658	0.0057	3.77643468
	6	10.5638	0.0077	5.10149948
	7	10.5619	0.0096	6.36031104
	8	10.5593	0.0122	8.08289528
	10	10.5545	0.0170	11.2630508
	12	10.5500	0.0215	14.2444466
	14.25	10.5443	0.0272	18.02088128
	16	10.5404	0.0311	20.60475764

Table B.16 - Erosion data generated for specimens 16A and 16B

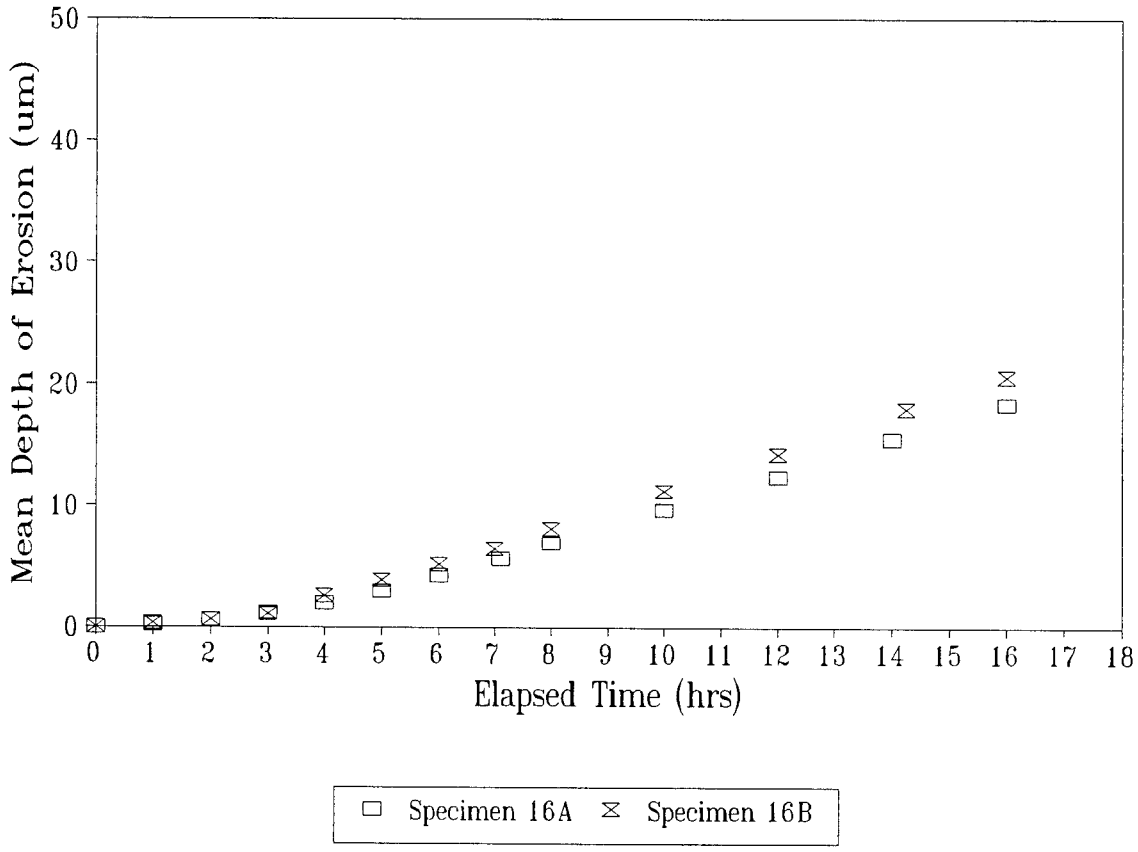

Figure B.16 - Erosion curves for specimens 16A and 16B.

Sample Identification	Experimental Test Data			
	Elapsed Time (hrs)	Specimen Mass (g)	Cumulative Mass Loss (g)	Mean Depth of Erosion (μm)
17A	0	10.8404	0.0000	0
	1.08	10.8400	0.0004	0.26501296
	2.08	10.8382	0.0022	1.45757128
	3.08	10.8356	0.0048	3.18015552
	4.10	10.8326	0.0078	5.16775272
	5.08	10.8295	0.0109	7.22160316
	6.08	10.8268	0.0136	9.01044064
	7.30	10.8233	0.0171	11.32930404
	8.08	10.8209	0.0195	12.9193818
	10.08	10.8148	0.0256	16.96082944
	12.08	10.8095	0.0309	20.47225116
	14.08	10.8034	0.0370	24.5136988
	16.08	10.7977	0.0427	28.29013348
17B	0	10.8391	0.0000	0
	1.2	10.8384	0.0007	0.46377268
	2	10.8373	0.0018	1.19255832
	3	10.8354	0.0037	2.45136988
	4	10.8327	0.0064	4.24020736
	5	10.8297	0.0094	6.22780456
	6	10.8269	0.0122	8.08289528
	7	10.8239	0.0152	10.07049248
	8	10.8209	0.0182	12.05808968
	10	10.8147	0.0244	16.16579056
	12	10.8091	0.0300	19.875972
	14	10.8035	0.0356	23.58615344
	16	10.7978	0.0413	27.36258812

Table B.17 - Erosion data generated for specimens 17A and 17B

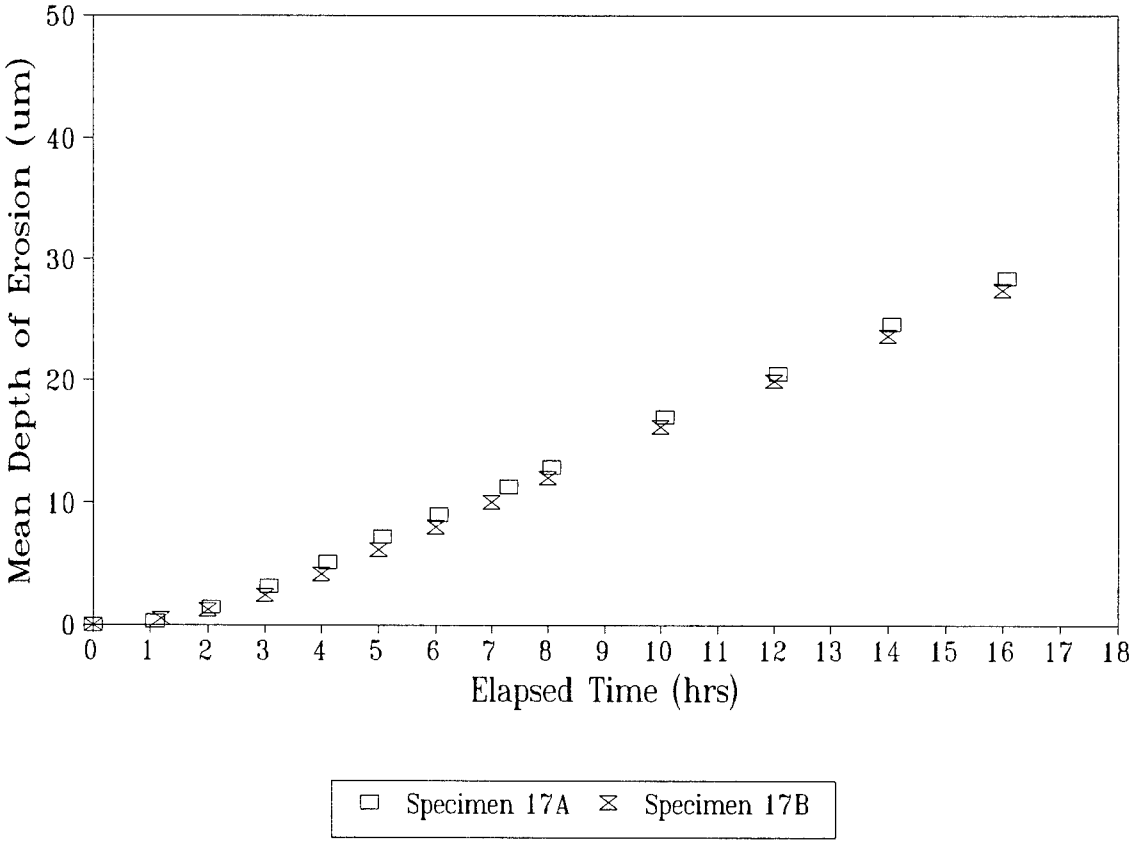

Figure B.17 - Erosion curves for specimens 17A and 17B.

Sample Identification	Experimental Test Data			
	Elapsed Time (hrs)	Specimen Mass (g)	Cumulative Mass Loss (g)	Mean Depth of Erosion (μm)
19A	0	10.9637	0.0000	0
	1	10.9626	0.0011	0.72878564
	2	10.9558	0.0079	5.23400596
	3	10.9471	0.0166	10.99803784
	4	10.9388	0.0249	16.49705676
	5	10.9311	0.0326	21.59855624
	6	10.9224	0.0413	27.36258812
	7	10.9136	0.0501	33.19287324
	9.36	10.8933	0.0704	46.64228096
	11.2	10.8784	0.0853	56.51401372
	13.06	10.8628	0.1009	66.84951916
	15.06	10.8485	0.1152	76.32373248
	16.06	10.8418	0.1219	80.76269956
19B	0	10.9855	0.0000	0
	1	10.9832	0.0023	1.52382452
	2	10.9760	0.0095	6.2940578
	3	10.9669	0.0186	12.32310264
	4	10.9582	0.0273	18.08713452
	5	10.9493	0.0362	23.98367288
	6	10.9408	0.0447	29.61519828
	7	10.9324	0.0531	35.18047044
	8	10.9227	0.0628	41.60703472
	10	10.9047	0.0808	53.53261792
	12	10.8874	0.0981	64.99442844
	14	10.8713	0.1142	75.66120008
	16	10.8555	0.1300	86.129212

Table B.18 - Erosion data generated for specimens 19A and 19B

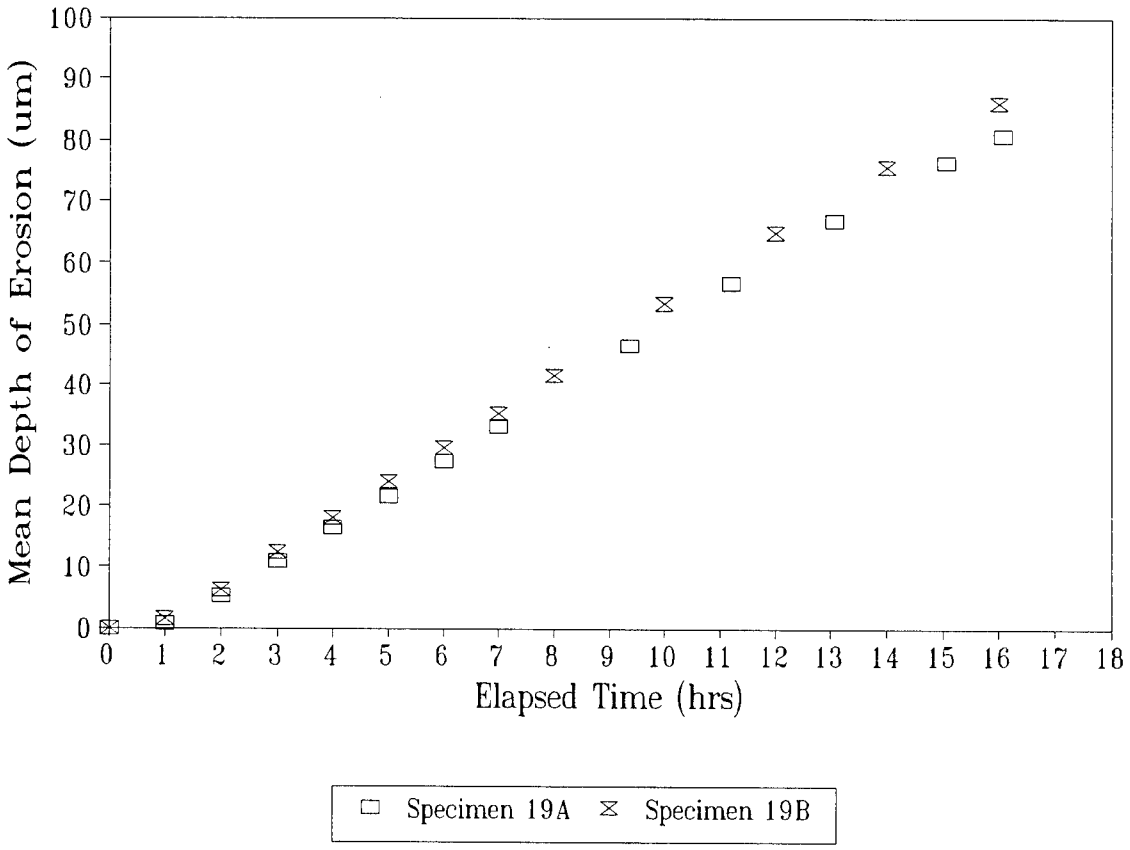

Figure B.18 - Erosion curves for specimens 19A and 19B.

Sample Identification	Experimental Test Data			
	Elapsed Time (hrs)	Specimen Mass (g)	Cumulative Mass Loss (g)	Mean Depth of Erosion (μm)
20A	0	10.7194	0.0000	0
	1	10.7192	0.0002	0.13250648
	2	10.7179	0.0015	0.9937986
	3	10.7164	0.0030	1.9875972
	4	10.7142	0.0052	3.44516848
	5	10.7124	0.0070	4.6377268
	6	10.7105	0.0089	5.89653836
	7.15	10.7076	0.0118	7.81788232
	8	10.7054	0.0140	9.2754536
	10	10.7009	0.0185	12.2568494
	12	10.6967	0.0227	15.03948548
	14	10.6928	0.0266	17.62336184
	16	10.6881	0.0313	20.73726412
20B	0	10.7326	0.0000	0
	1	10.7320	0.0006	0.39751944
	2	10.7304	0.0022	1.45757128
	3	10.7287	0.0039	2.58387636
	4	10.7267	0.0059	3.90894116
	5	10.7246	0.0080	5.3002592
	6	10.7231	0.0095	6.2940578
	7	10.7206	0.0120	7.9503888
	8	10.7185	0.0141	9.34170684
	10.15	10.7139	0.0187	12.38935588
	12	10.7102	0.0224	14.84072576
	14	10.7059	0.0267	17.68961508
	16	10.7015	0.0311	20.60475764

Table B.19 - Erosion data generated for specimens 20A and 20B

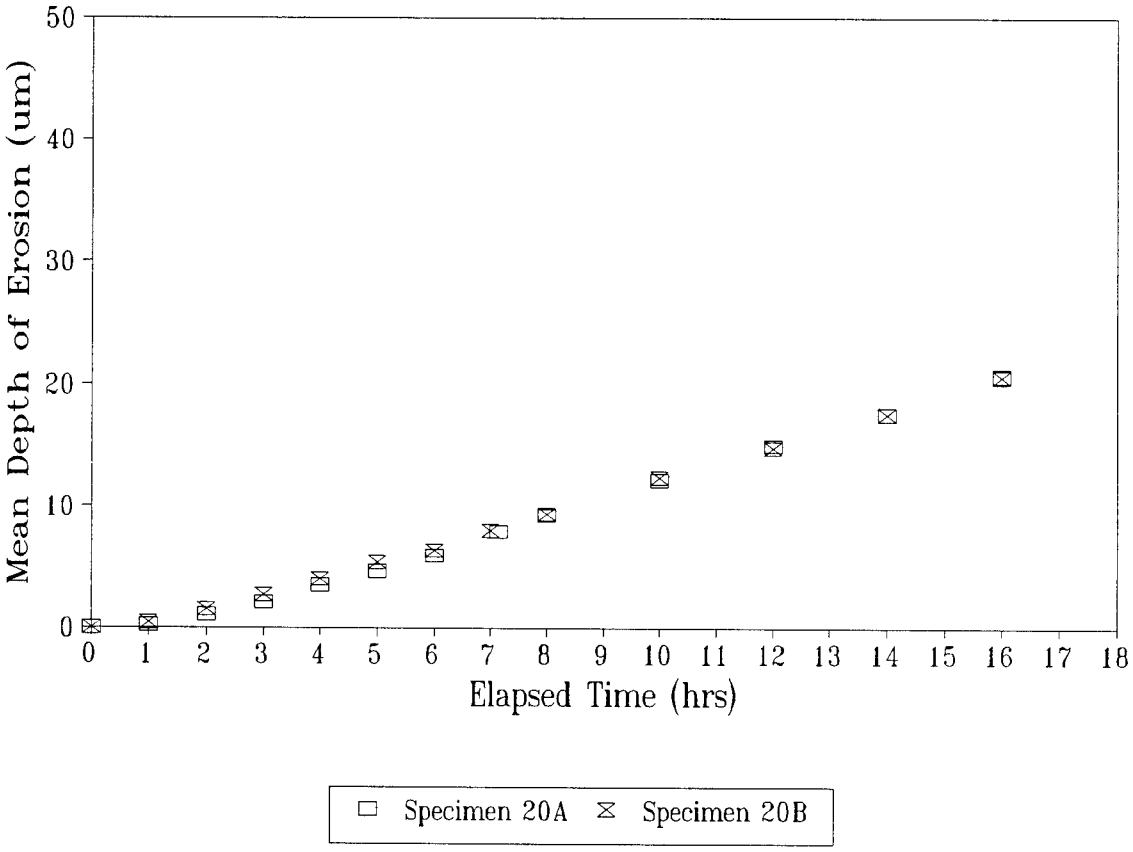

Figure B.19 - Erosion curves for specimens 20A and 20B.

Sample Identification	Experimental Test Data			
	Elapsed Time (hrs)	Specimen Mass (g)	Cumulative Mass Loss (g)	Mean Depth of Erosion (μm)
21A	0	10.7719	0.0000	0
	1	10.7713	0.0006	0.39751944
	2	10.7705	0.0014	0.92754536
	3	10.7687	0.0032	2.12010368
	4			
	5	10.7648	0.0071	4.70398004
	6	10.7625	0.0094	6.22780456
	7	10.7603	0.0116	7.68537584
	8	10.7577	0.0142	9.40796008
	10	10.7540	0.0179	11.85932996
	12	10.7486	0.0233	14.77447252
	14	10.7442	0.0277	18.35214748
	16	10.7397	0.0322	21.33354328
21B	0	10.8080	0.0000	0
	1	10.8073	0.0007	0.46377268
	2.1	10.8063	0.0017	1.12630508
	3	10.8045	0.0035	2.3188634
	4	10.8024	0.0056	3.71018144
	5	10.8003	0.0077	5.10149948
	6	10.7979	0.0101	6.69157724
	7	10.7955	0.0125	8.281655
	8	10.7930	0.0150	9.937986
	10.2	10.7874	0.0206	13.64816744
	12	10.7834	0.0246	16.29829704
	14	10.7783	0.0297	19.67721228
	16	10.7738	0.0342	22.65860808

Table B.20 - Erosion data generated for specimens 21A and 21B

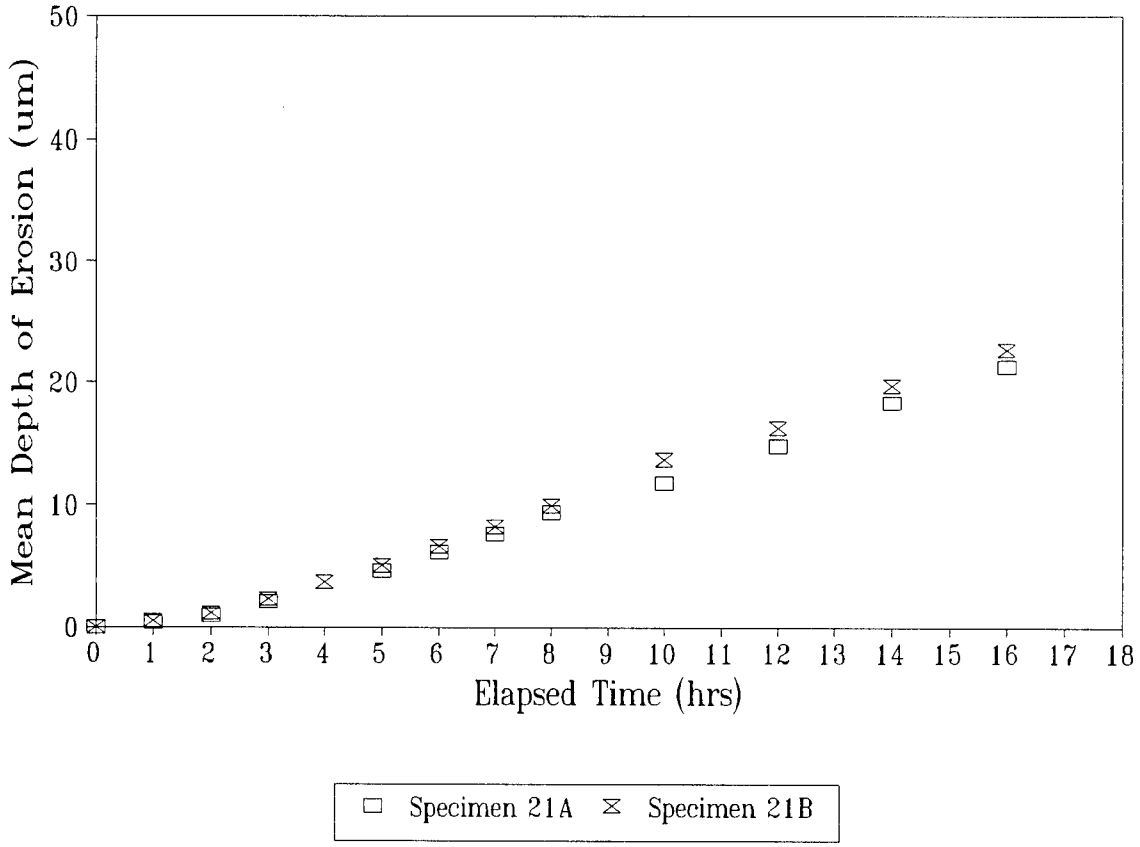

Figure B.20 - Erosion curves for specimens 21A and 21B.

Sample Identification	Experimental Test Data			
	Elapsed Time (hrs)	Specimen Mass (g)	Cumulative Mass Loss (g)	Mean Depth of Erosion (μm)
22A	0	10.8315	0.0000	0
	1	10.8310	0.0005	0.3312662
	2.1	10.8300	0.0015	0.9937986
	3	10.8280	0.0035	2.3188634
	4	10.8260	0.0055	3.6439282
	5	10.8237	0.0078	5.16775272
	6	10.8208	0.0107	7.08909668
	7	10.8187	0.0128	8.48041472
	8	10.8161	0.0154	10.20299896
	10	10.8108	0.0207	13.71442068
	12	10.8052	0.0263	17.42460212
	14	10.8000	0.0315	20.8697706
	16	10.7943	0.0372	24.64620528
22B	0	10.8334	0.0000	0
	1	10.8328	0.0006	0.39751944
	2	10.8313	0.0021	1.39131804
	3	10.8291	0.0043	2.84888932
	4.5	10.8258	0.0076	5.03524624
	5.5	10.8228	0.0106	7.02284344
	6.5	10.8204	0.0130	8.6129212
	7.6	10.8175	0.0159	10.53426516
	8.7	10.8144	0.0190	12.5881156
	10.7	10.8090	0.0244	16.16579056
	12.8	10.8035	0.0299	19.80971876
	14.8	10.7987	0.0347	22.98987428
	16.7	10.7917	0.0417	27.62760108

Table B.21 - Erosion data generated for specimens 22A and 22B

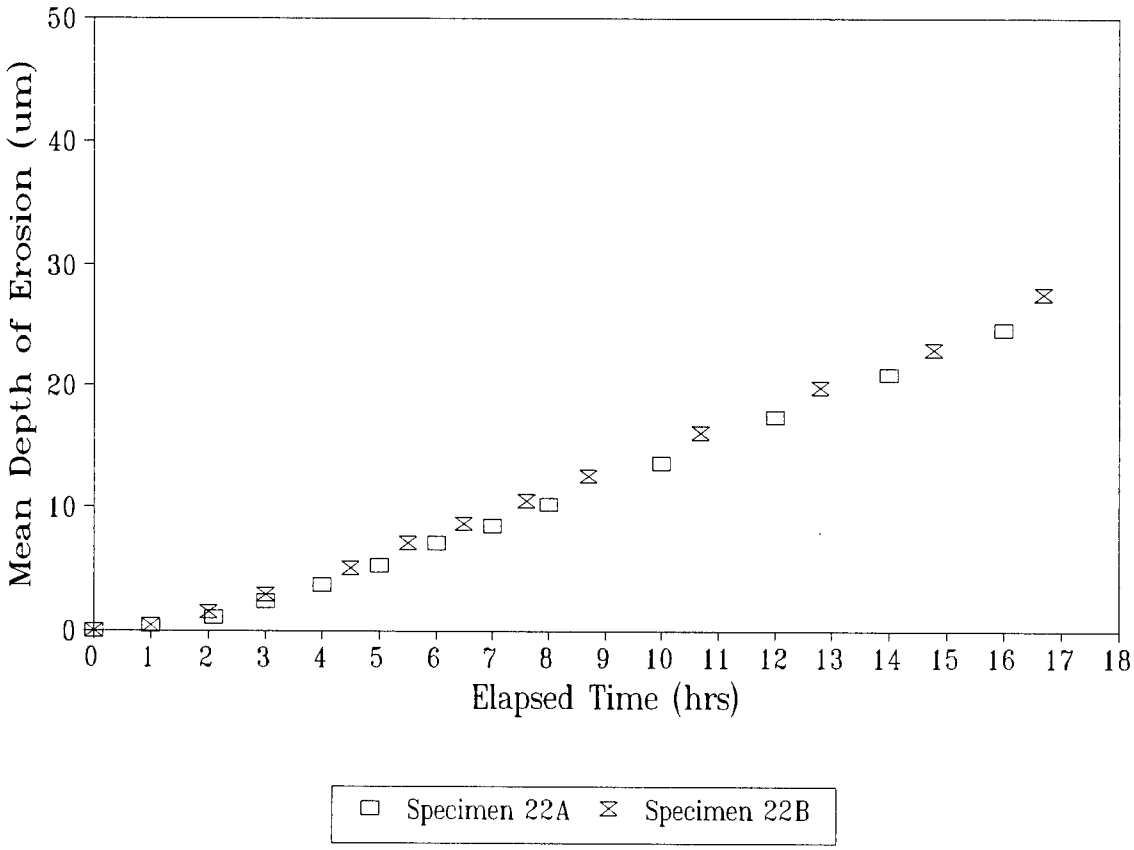

Figure B.21 - Erosion curves for specimens 22A and 22B.

Sample Identification	Experimental Test Data			
	Elapsed Time (hrs)	Specimen Mass (g)	Cumulative Mass Loss (g)	Mean Depth of Erosion (μm)
23A	0	10.7452	0.0000	0
	1	10.7444	0.0008	0.53002592
	2	10.7420	0.0032	2.12010368
	3	10.7375	0.0077	5.10149948
	4	10.7337	0.0115	7.6191226
	5	10.7295	0.0157	10.40175868
	6	10.7254	0.0198	13.11814152
	7	10.7213	0.0239	15.83452436
	8	10.7175	0.0277	18.35214748
	10	10.7090	0.0362	23.98367288
	12	10.7011	0.0441	29.21767884
	14.33	10.6909	0.0543	35.97550932
	16	10.6843	0.0609	40.34822316
23B	0	10.7177	0.0000	0
	1	10.7171	0.0006	0.39751944
	2	10.7145	0.0032	2.12010368
	3	10.7106	0.0071	4.70398004
	4	10.7069	0.0108	7.15534992
	5	10.7027	0.0150	9.937986
	6	10.6987	0.0190	12.5881156
	7	10.6948	0.0229	15.17199196
	8	10.6909	0.0268	17.75586832
	10	10.6831	0.0346	22.92362104
	12	10.6752	0.0425	28.157627
	14	10.6674	0.0503	33.32537972
	16	10.6591	0.0586	38.82439864

Table B.22 - Erosion data generated for specimens 23A and 23B

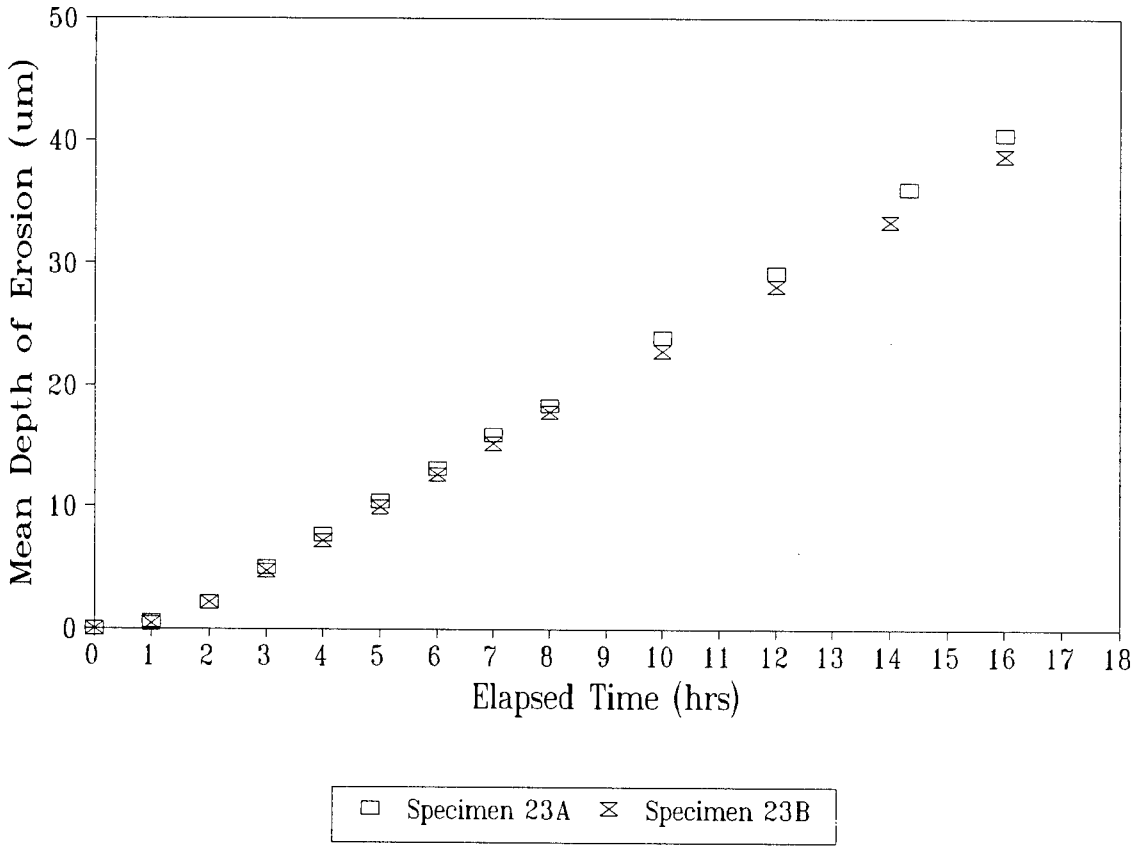

Figure B.22 - Erosion curves for specimens 23A and 23B.

Sample Identification	Experimental Test Data			
	Elapsed Time (hrs)	Specimen Mass (g)	Cumulative Mass Loss (g)	Mean Depth of Erosion (μm)
25A	0	10.8124	0.0000	0
	1	10.8120	0.0004	0.26501296
	2	10.8113	0.0011	0.72878564
	3	10.8097	0.0027	1.78883748
	4	10.8080	0.0044	2.91514256
	5	10.8061	0.0063	4.17395412
	6	10.8042	0.0082	5.43276568
	7.2	10.8014	0.0110	7.2878564
	8	10.7997	0.0127	8.41416148
	10	10.7958	0.0166	10.99803784
	12	10.7919	0.0205	13.5819142
	14	10.7877	0.0247	16.36455028
	16	10.7833	0.0291	19.27969284
25B	0			
	1			
	2			
	3			
	4			
	5			
	6			
	7			
	8			
	10			
	12			
	14			
	16			

Table B.23 - Erosion data generated for specimens 25A and 25B

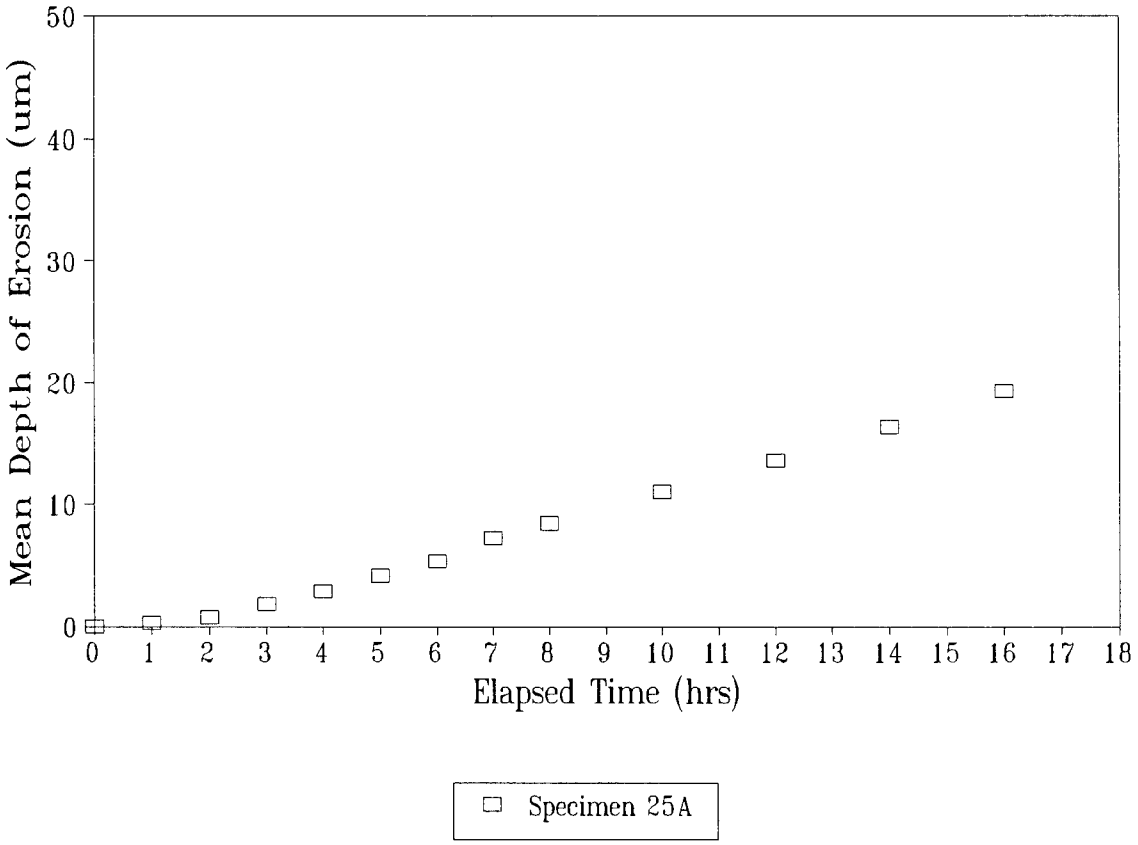

Figure B.23 - Erosion curve for specimen 25A.

Sample Identification	Experimental Test Data			
	Elapsed Time (hrs)	Specimen Mass (g)	Cumulative Mass Loss (g)	Mean Depth of Erosion (μm)
30A	0	10.5634	0.0000	0
	1	10.5627	0.0005	0.3312662
	2	10.5607	0.0025	1.656331
	3	10.5578	0.0056	3.71018144
	4	10.5544	0.0090	5.9627916
	5	10.5513	0.0121	8.01664204
	6	10.5476	0.0158	10.46801192
	7	10.5449	0.0185	12.2568494
	8	10.5417	0.0217	14.37695308
	10	10.5349	0.0285	18.8821734
Specimen	12			
fatigued on	14			
first thread	16			
30B	0	10.6258	0.0000	0
	1	10.6252	0.0006	0.39751944
	2	10.6236	0.0022	1.45757128
	3	10.6209	0.0049	3.24640876
	4	10.6185	0.0073	4.83648652
Specimen	5			
fatigued on	6			
first thread	7			
	8			
	10			
	12			
	14			
	16			

Table B.24 - Erosion data generated for specimens 30A and 30B

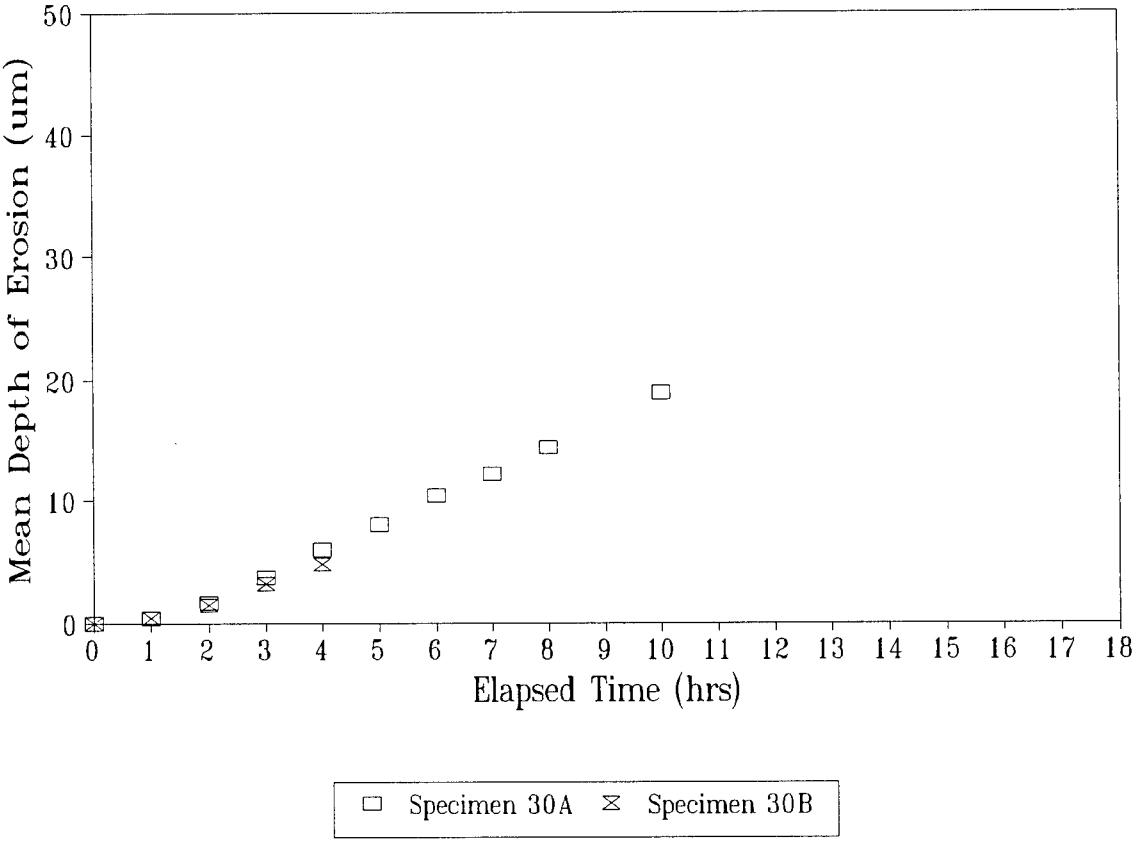

Figure B.24 - Erosion curves for specimens 30A and 30B.

Sample Identification	Experimental Test Data			
	Elapsed Time (hrs)	Specimen Mass (g)	Cumulative Mass Loss (g)	Mean Depth of Erosion (μm)
32A	0	10.9808	0.0000	0
	1	10.9794	0.0014	0.92754536
	2	10.9739	0.0069	4.57147356
	3	10.9673	0.0135	8.9441874
	4	10.9612	0.0196	12.98563504
	5	10.9546	0.0262	17.35834888
	6	10.9483	0.0325	21.532303
	7	10.9418	0.0390	25.8387636
	8	10.9360	0.0448	29.68145152
	10	10.9238	0.0570	37.7643468
	12	10.9118	0.0690	45.7147356
	14	10.8995	0.0813	53.86388412
	16	10.8875	0.0933	65.78946732
32B	0	10.9604	0.0000	0
	1			
	2	10.9540	0.0064	4.24020736
	3	10.9480	0.0124	8.21540176
	4	10.9423	0.0181	11.99183644
	5	10.9360	0.0244	16.16579056
	6	10.9302	0.0302	20.00847848
	7	10.9248	0.0356	23.58615344
	8	10.9207	0.0397	26.30253628
	10	10.9065	0.0539	35.71049636
	12	10.8944	0.0660	43.7271384
	14	10.8825	0.0779	51.61127396
	16	10.8702	0.0902	59.76042248

Table B.25 - Erosion data generated for specimens 32A and 32B

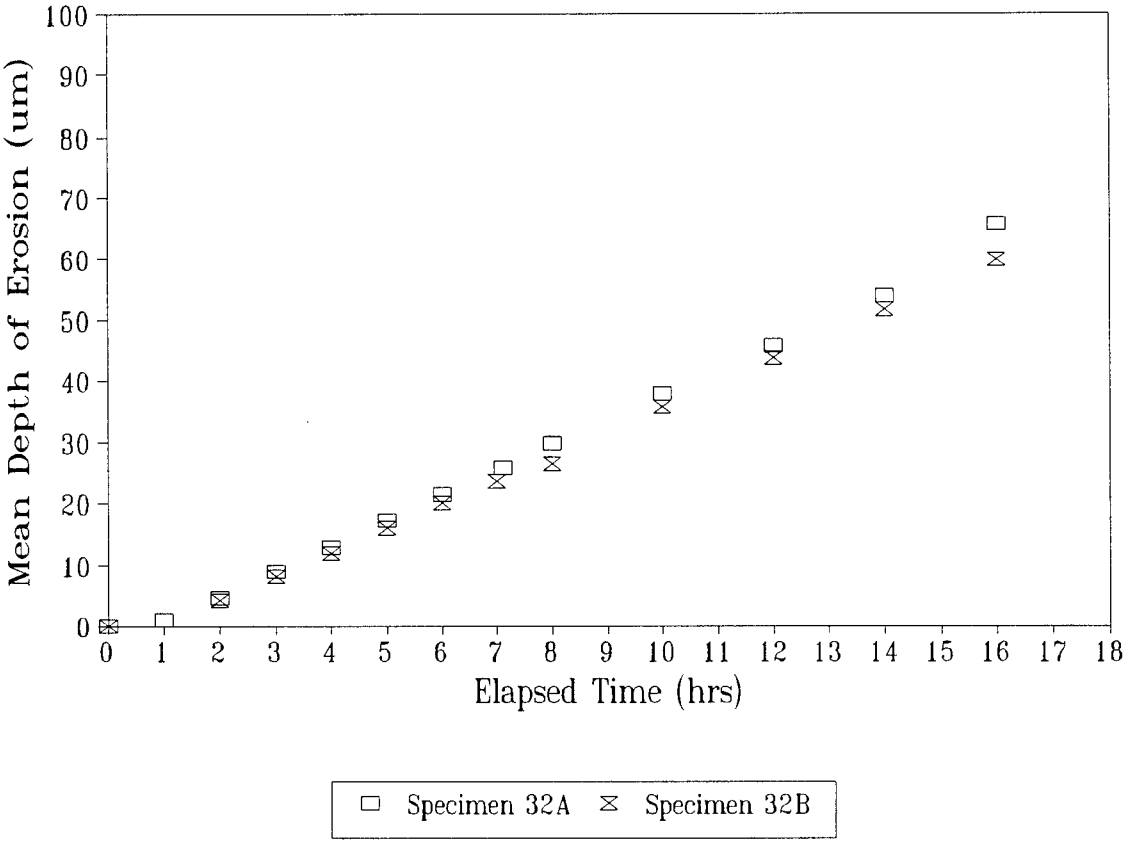

Figure B.25 - Erosion curves for specimens 32A and 32B.

Sample Identification	Experimental Test Data			
	Elapsed Time (hrs)	Specimen Mass (g)	Cumulative Mass Loss (g)	Mean Depth of Erosion (μm)
33A	0	10.9560	0.0000	0
	1	10.9553	0.0007	0.46377268
	2	10.9508	0.0052	3.44516848
	3	10.9453	0.0107	7.08909668
	4	10.9402	0.0158	10.46801192
	5.17	10.9342	0.0218	14.44320632
	6	10.9294	0.0266	17.62336184
	7	10.9249	0.0311	20.60475764
	8	10.9195	0.0365	24.1824326
	10	10.9097	0.0463	30.67525012
	12	10.8991	0.0569	37.69809356
	14	10.8890	0.0670	44.3896708
	16	10.8788	0.0772	51.14750128
33B	0	10.9323	0.0000	0
	1.1	10.9309	0.0014	0.92754536
	2	10.9270	0.0053	3.51142172
	3	10.9225	0.0098	6.49281752
	4	10.9168	0.0155	10.2692522
	5	10.9115	0.0208	13.78067392
	6	10.9060	0.0263	17.42460212
	7	10.9009	0.0314	20.80351736
	8	10.8951	0.0372	24.64620528
Specimen fatigued on first thread	10			
	12			
	14			
	16			

Table B.26 - Erosion data generated for specimens 33A and 33B

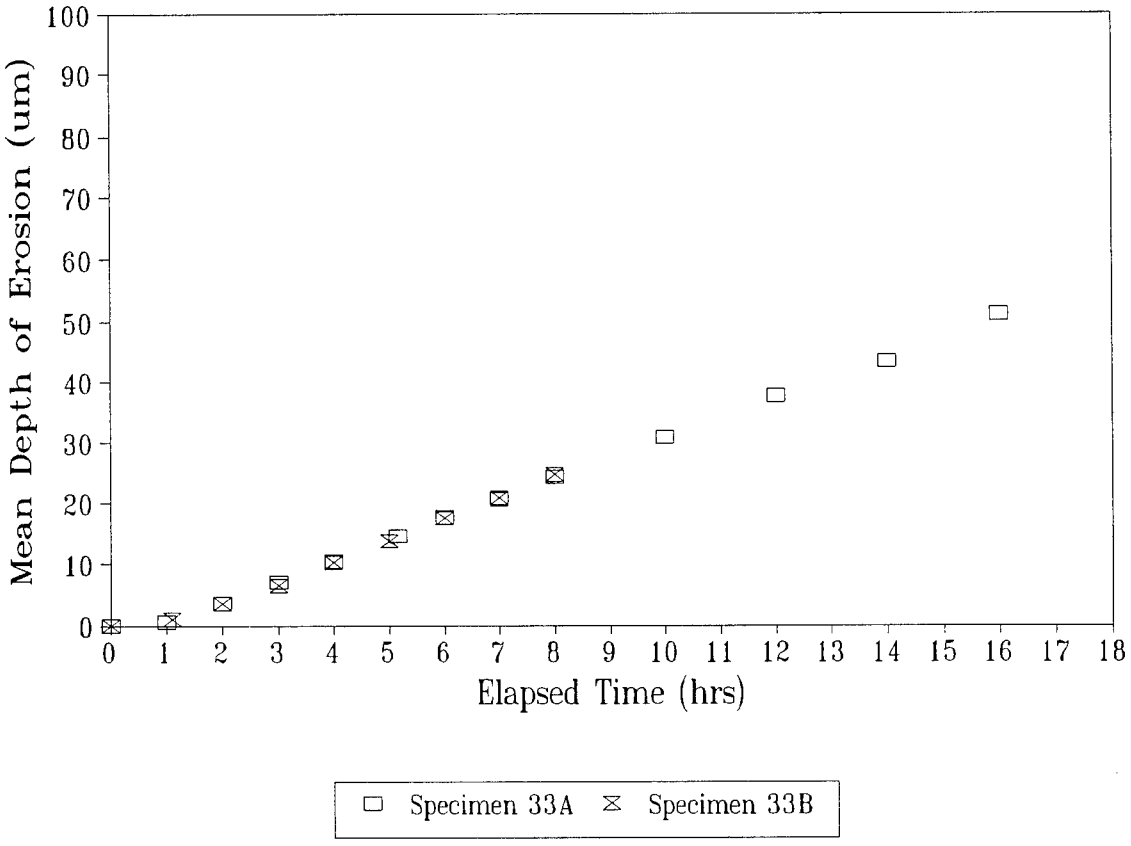

Figure B.26 - Erosion curves for specimens 33A and 33B.

UNCLASSIFIED

SECURITY CLASSIFICATION OF FORM
(highest classification of Title, Abstract, Keywords)

DOCUMENT CONTROL DATA

(Security classification of title, body of abstract and indexing annotation must be entered when the overall document is classified)

1. ORIGINATOR (The name and address of the organization preparing the document. Organizations for whom the document was prepared, e.g. Establishment sponsoring a contractor's report, or tasking agency, are entered in section 8.)

FACTS Engineering Inc.
P.O. Box 20039
Halifax, Nova Scotia, Canada, B3K 2K9.

2. SECURITY CLASSIFICATION (Overall security of the document including special warning terms if applicable.)

UNCLASSIFIED

3. TITLE (The complete document title as indicated on the title page. Its classification should be indicated by the appropriate abbreviation (S,C.R or U) in parentheses after the title.)

Evaluation of Cavitation Erosion Behavior of Laser Surface Melted Experimental Nickel Aluminum Bronze.

4. AUTHORS (Last name, first name, middle initial. If military, show rank, e.g. Doe, Maj. John E.)

K.J. KarisAllen and C.A. Taweel

5. DATE OF PUBLICATION (Month and year of publication of document.)

May 1997

6a. NO. OF PAGES (Total containing information. Include Annexes, Appendices, etc.)

75

6b. NO. OF REFS. (Total cited in document.)

3

6. DESCRIPTIVE NOTES (The category of the document, e.g. technical report, technical note or memorandum. If appropriate, enter the type of report, e.g. interim, progress, summary, annual or final. Give the inclusive dates when a specific reporting period is covered.)

Contractor Report (Final)

8. SPONSORING ACTIVITY (The name of the department project office or laboratory sponsoring the research and development. include the address.)

Defence Research Establishment Atlantic
P.O. Box 1012, Dartmouth, N.S. B2Y 3Z7

9a. PROJECT OR GRANT NUMBER (If appropriate, the applicable research and development project or grant number under which the document was written. Please specify whether project or grant.)

1 gh-16

9b. CONTRACT NUMBER (If appropriate, the applicable number under which the document was written.)

DREA CR 97/419

10a. ORIGINATOR'S DOCUMENT NUMBER (The official document number by which the document is identified by the originating activity. This number must be unique to this document.)

N/A

10b. OTHER DOCUMENT NUMBERS (Any other numbers which may be assigned this document either by the originator or by the sponsor.)

W7707-6-4270/001/HAL

11. DOCUMENT AVAILABILITY (Any limitations on further dissemination of the document, other than those imposed by security classification)

(X) Unlimited distribution
( ) Distribution limited to defence departments and defence contractors; further distribution only as approved
( ) Distribution limited to defence departments and Canadian defence contractors; further distribution only as approved
( ) Distribution limited to government departments and agencies; further distribution only as approved
( ) Distribution limited to defence departments; further distribution only as approved
( ) Other (please specify):

12. DOCUMENT ANNOUNCEMENT (Any limitation to the bibliographic announcement of this document. This will normally correspond to the Document Availability (11). However, where further distribution (beyond the audience specified in 11) is possible, a wider announcement audience may be selected.)

Limited to DND

13. ABSTRACT (a brief and factual summary of the document. It may also appear elsewhere in the body of the document itself. It is highly desirable that the abstract of classified documents be unclassified. Each paragraph of the abstract shall begin with an indication of the security classification of the information in the paragraph (unless the document itself is unclassified) represented as (S), (C), (R), or (U). It is not necessary to include here abstracts in both official languages unless the text is bilingual).

A series of laser surface melted experimental nickel aluminum bronze coupons have been evaluated for cavitation erosion resistance. Duplicate specimens of twenty five differing alloy compositions have been tested in accordance with ASTM G-32. For the materials tested, test results indicate that alloy chemistries with more than 10.7 wt percent Al produce the best resistance to cavitation erosion. The cavitation resistance of alloys with less than 10.7 percent Al can be improved through the addition of Cr. The analysis also indicates that the linear extrapolation method recommended in ASTM G-32 may produce non conservative incubation times for laser surface melted specimens with above average erosion performance.

14. KEYWORDS, DESCRIPTORS or IDENTIFIERS (technically meaningful terms or short phrases that characterize a document and could be helpful in cataloguing the document. They should be selected so that no security classification is required. Identifiers, such as equipment model designation, trade name, military project code name, geographic location may also be included. If possible keywords should be selected from a published thesaurus. e.g. Thesaurus of Engineering and Scientific Terms (TEST) and that thesaurus-identified. If it not possible to select indexing terms which are Unclassified, the classification of each should be indicated as with the title).

Laser Welding
Cavitation Erosion
Nickel Aluminum Bronze
Alloying
Chromium
Titanium
Zirconium